energies

MDPI

Review

Insights into Enhancing Electrochemical Performance of Li-Ion Battery Anodes via Polymer Coating

Mozaffar Abdollahifar [1,2,*], Palanivel Molaiyan [3], Milena Perovic [1,2] and Arno Kwade [1,2]

[1] Institute for Particle Technology, Technische Universität Braunschweig, Volkmaroder Str. 5, 38104 Braunschweig, Germany
[2] Battery LabFactory Braunschweig (BLB), Technische Universität Braunschweig, Langer Kamp 19, 38106 Braunschweig, Germany
[3] Research Unit of Sustainable Chemistry, University of Oulu, 90570 Oulu, Finland
* Correspondence: m.abdollahifar@tu-bs.de

Abstract: Due to the ever-growing importance of rechargeable lithium-ion batteries, the development of electrode materials and their processing techniques remains a hot topic in academia and industry. Even the well-developed and widely utilized active materials present issues, such as surface reactivity, irreversible capacity in the first cycle, and ageing. Thus, there have been many efforts to modify the surface of active materials to enhance the electrochemical performance of the resulting electrodes and cells. Herein, we review the attempts to use polymer coatings on the anode active materials. This type of coating stands out because of the possibility of acting as an artificial solid electrolyte interphase (SEI), serving as an anode protective layer. We discuss the prominent examples of anodes with different mechanisms: intercalation (graphite and titanium oxides), alloy (silicon, tin, and germanium), and conversion (transition metal oxides) anodes. Finally, we give our perspective on the future developments in this field.

Keywords: polymer coating; anode materials; lithium-ion batteries; artificial solid electrolyte interphase

Citation: Abdollahifar, M.; Molaiyan, P.; Perovic, M.; Kwade, A. Insights into Enhancing Electrochemical Performance of Li-Ion Battery Anodes via Polymer Coating. *Energies* **2022**, *15*, 8791. https://doi.org/10.3390/en15238791

Academic Editor: Seung-Wan Song

Received: 2 October 2022
Accepted: 16 November 2022
Published: 22 November 2022

1. Introduction

The development of rechargeable lithium-ion batteries (LIBs) began in the early 1990s and received remarkable attention, as they are employed in many modern portable electronic devices, as well as hybrid electric vehicles (HEVs) and electric vehicles (EVs) because of their high energy densities [1]. The progress is very fast regarding the development of new active anode and cathode materials, electrolyte formulation, electrode composition, and cell design with consideration of safety and costs [2,3]. The interest in developing active materials for LIBs has been considerably increasing to enhance specific capacity and enable higher rate capability and long cycle life stability—the critical parameters for practical applications. Various material modification methods have been introduced in academia and industry to improve the general properties of active materials without changing the elemental or crystal structure, and thereby, the intrinsic properties. One of the well-known methods is surface architecture, which represents surface coating and etching, which protects the active material particles from direct contact with the electrolyte. In LIBs containing liquid (or polymer) electrolytes, the electrode surface is covered by a passivating layer called the solid electrolyte interface (SEI) on the anode materials and the cathode electrolyte interface (CEI) [4] on the cathode particles. The SEI in particular has been regarded as a crucial interface in the battery related to the capacity fade, cycle life, and other key performance parameters. The SEI has a protective role, blocking the electrons that could further reduce the electrolyte, but it also consumes the valuable electrolyte and Li-ions, leading to irreversible capacity loss [5,6]. During the first few cycles, the SEI film forms from electrolyte decomposition and reduction reactions with the lithium salts on the anode particle surface [7]. However, the SEI film is usually not stable, particularly for anode materials with massive volume

expansion during the lithiation step. Therefore, the electrolyte ions are consumed over the cycles, resulting in capacity degradation [8].

Coating the thin layer of "protective" material onto the active material particle can increase its micro-structure stability, resulting in improved electrochemical properties. Many modifications to the electrode [9–13] and active material particles have been investigated, such as surface modification by carbon, metal oxides, and polymers [14–24]. Coatings consisting of inorganic materials, such as Al_2O_3, MgO, ZrO_2, SiO_2, TiO_2, and others, commonly provide a Li^+-conducting protective layer on the active material, which reduces the chemical reaction between the active material and the electrolyte. However, their deposition usually requires a high-temperature treatment, and the formation of uniformly distributed coating is very challenging.

The SEI should allow the rapid Li-ion transfer between the electrolyte and the electrode without blocking the electron pathway on the electrode current collector interface. Ideally, this layer should self-heal when the changes in the electrode surface occur due to volume expansion. A thin polymer layer on active anode materials can theoretically fulfill these criteria and could act as an artificial SEI. The properties of this layer, such as its thickness, ion-diffusion capability, chemical composition, and mechanical properties, are vital for having a stable electrode. In this review paper, we attempt to analytically address the progress of polymer coating on anode electrodes/particles to enhance the electrochemical performance of LIBs.

2. Polymer Coating on Anode Materials

In the following sections, we discuss the effect of polymer coating on the electrochemical performance and morphology of different anode materials with mainly three different electrochemical (de)lithiation mechanisms, the advantages and drawbacks for these anode materials are summarized in Table 1:

- Intercalation anodes, such as Graphite (Gr) and Titanium oxides.
- Alloy anodes, for instance, Silicon (Si), Germanium (Ge), and Tin (Sn).
- Conversion anodes, for example, transition metal oxides (Fe_3O_4, Co_3O_4, CuO, etc.).

Table 1. An overview of the (dis)advantages of different types of anodes.

Types of Anodes	Benefits	Drawbacks
Intercalation-type anodes	Low-cost materials, high electronic conductivity, good safety for Ti-based anodes, long cycle life, high power capability	Low specific capacity, safety issue for Gr, low energy density
Alloy-type anodes	High specific capacity, good safety, low-cost materials and abundance for Si, high energy density	Large volume changes, low electronic conductivity, poor CE, poor cycling
Conversion-type anodes	High specific capacity, low-cost materials, low operation potential	Poor CE, unstable SEI, poor cycling

Figure 1 illustrates the advantages and drawbacks of these three types of materials and the connection between working potentials and the specific capacity of the anode materials [25]. Generally, depending on the anode active material, polymer coating on the particles could help resolve some critical challenges, such as poor cycle life and C-rate capability, low Coulombic efficiency (CE), unstable SEI, and high irreversible capacity, which will be addressed here in detail for the specific polymers and anode materials.

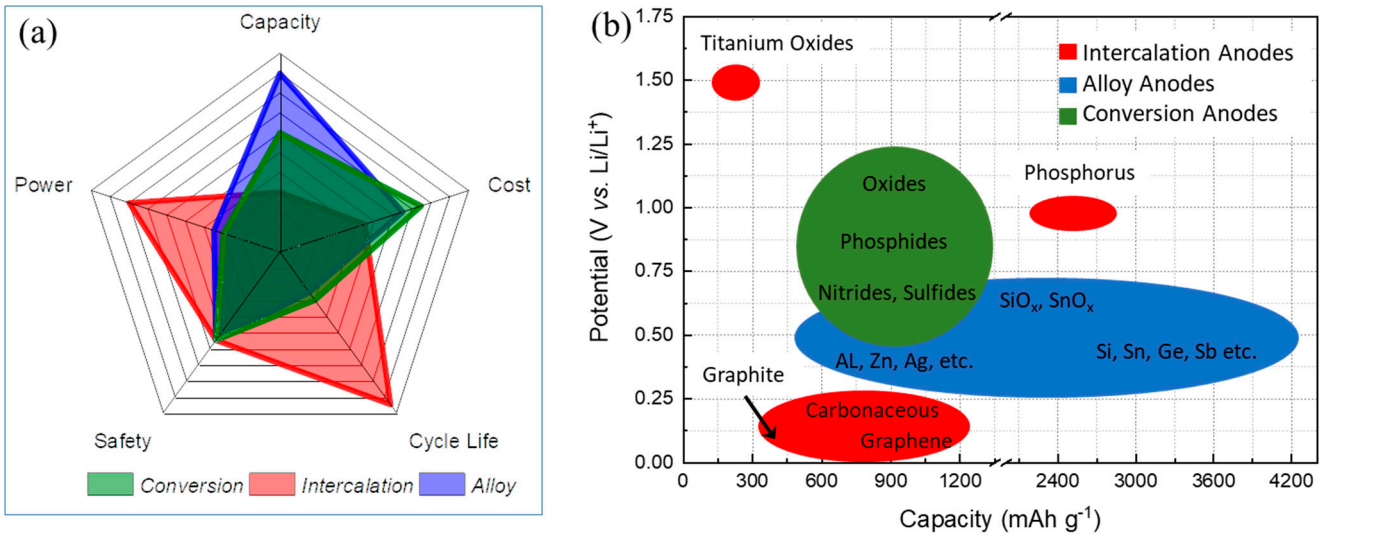

Figure 1. Anode active materials with three different primary electrochemical (de)lithiation mechanisms: (**a**) Radar plot comparing five critical categories of capacity, cost, cycle life, safety, and power. (**b**) Schematic illustration comparing potential vs. capacity of certain anode materials.

A thin polymer layer on active anode materials could act as an artificial SEI. This layer can be fabricated for mechanical flexibility to maintain the passivation of active anode materials. The polymer film could be synthesized via different techniques [26–39]. Generally, thin polymer films could accommodate volume expansion (unlike glass or ceramic layers) while simultaneously demonstrating good chemical and structural stabilities during (de)lithiation processes. The polymer film thickness is typically about 2–25 nm [10,40–53].

Conductive polymers are attractive additive materials for LIBs because of their outstanding electrochemical properties: enhancing the electronic conductivity, inhibiting the phase transition, increasing structural stability, decreasing active material dissolution, leading to a remarkable improvement in reversible capacity, rate capability, and cycle stability. Conductive polymers, such as polypyrrole (PPy) [44], polyaniline (PANi) [54], poly(3,4-ethylenedioxythiophene) (PEDOT) [55], PEDOT:poly(styrenesulfonate) (PEDOT:PSS) [31], and polythiophene (PT) [33], but also other polymers, such as polyvinylidene fluoride (PVDF) [12,32] and Polydopamine (PDA) [56], have been used as attractive coating agents for active anode materials to improve the mechanical flexibility and the electrochemical performance of LIBs. Figure 2 demonstrates the contribution of polymers reported in the literature chosen here for coating active anode materials. The category "others" comprises the literature using polyvinylpyrrolidone and polyacrylonitrile [49], poly(1,3,5,7-tetravinyl-1,3,5,7-tetramethylcyclotetrasiloxane) [51], poly(vinyl alcohol) [52,57], polyether, polyethylene glycol tert -octylphenylether and polymer polyallyl amine [17], poly(diallyl dimethylammonium chloride) and poly(sodium 4-styrenesulfonate) [58], polyacrylic acid and polymethacrylic acid [9], PVDF [12,32], 1,3,5-trivinyl-1,3,5-trimethylcyclotrisiloxane [13], PEDOT:PSS [31,59], PDA [56], poly(dimethyldiallylammonium chloride) and poly(methyl methacralate) (PMMA), poly(sodium-p-styrenesulfonate) [60], 1,3,5-trimethylcyclotrisiloxane (V3D3) [13] and poly(ethylene oxide) [61]. These polymers may serve as a host for Li-ion (de)intercalation and enhance the electron transfer in the electrode, particularly with the electrodeposition method. In the following sections, we will discuss the effects of polymer coating on the electrochemical performance of anode materials.

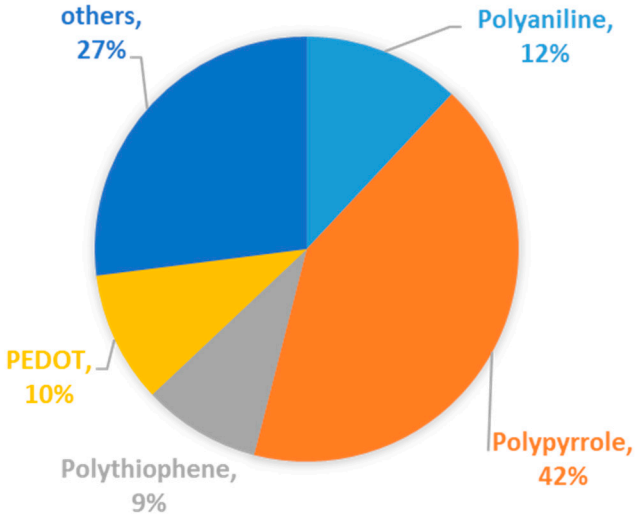

Figure 2. The percentage of various polymers (PPy, PEDOT, PT, PANi, and others) that have been used to coat anode materials so far reported in the literature.

3. Intercalation Anodes

3.1. Graphite (Gr)

Gr, as a state-of-the-art anode material of LIBs, has been investigated [62–64], and it has been on the market for almost three decades, since the beginning of the commercialization of LIBs. Although Gr has a low capacity, it is a reliable and stable anode material, but some significant challenges still remain:

- Rate capability: safety issues because of lithium (Li) plating on the electrode surface.
- First cycle irreversible capacity, or initial CE towing to the electrolyte decomposition, and therefore, the consumption of Li-ions as the charge carrier.
- Ageing, prompted by cycling and calendar ageing, and the resulting safety concerns because of the low (de)lithiation potential close to the Li plating.

These challenges potentially result in accelerated capacity fading. During recent years, many improvements have been made to Gr morphology and particle sizes, but there have also been extensive investigations into the functionalization of Gr-based anodes via polymer, carbon, and nano-oxide coating layers [9,12,13,38,39,65–72]. Surface modification of the Gr particles is one strategy to enhance the electrochemical performance and solve some of the challenges mentioned earlier [68]. The reported studies about polymer coating on Gr particles/electrodes of LIBs are discussed in the following paragraphs.

When an ethylene carbonate (EC)-based electrolyte is used, the stable SEI is formed during the first charging, enabling the reversible Li (de)intercalation [9,69,73]. However, these electrolytes are unsuitable for low operating temperatures. Propylene carbonate (PC) with low freezing temperature (−49 °C), higher ionic conductivity at low temperatures than EC electrolytes, and a high melting point (37 °C) is one of the alternatives for EC-based electrolytes and could be used in LIB applications. However, PC-based electrolytes experience a major drawback, since Li-ions solvated with PC molecules co-intercalate into crystalline Gr; this causes the exfoliation of graphene layers and the continuous decomposition of the electrolyte, low Columbic efficiency, and finally, capacity fading due to lack of a suitable SEI [74,75]. To address this issue, many electrolyte additives are studied to improve the electrochemical performance and formation of a stable SEI to only pass Li-ion without solvents [9]. Another approach to suppress the decomposition and co-intercalation of PC molecules is the surface modification of Gr using polymers [9,69,73]. Komaba et al. [9] have studied Gr electrode modification using polyacrylic acid (PAA), polymethacrylic acid (PMA), and polyvinyl alcohol (PVA) as binders to modify the electrode surface. The electrochemical properties of polymer-coated Gr as anodes of LIBs were investigated in $LiClO_4$ dissolved in PC (Figure 3). The sample using PAA did not show visible exfoliation of Gr after the first

cycle in $LiClO_4$ in PC, whereas for the sample with PVDF, a partial exfoliation of Gr was confirmed (Figure 3a,b). The polymer-coated Gr particles showed a thin SEI layer due to the enhanced SEI formation process caused by the interaction of oxygen in the polymers and Li-ions, resulting in a much better electrochemical performance (Figure 3c,d).

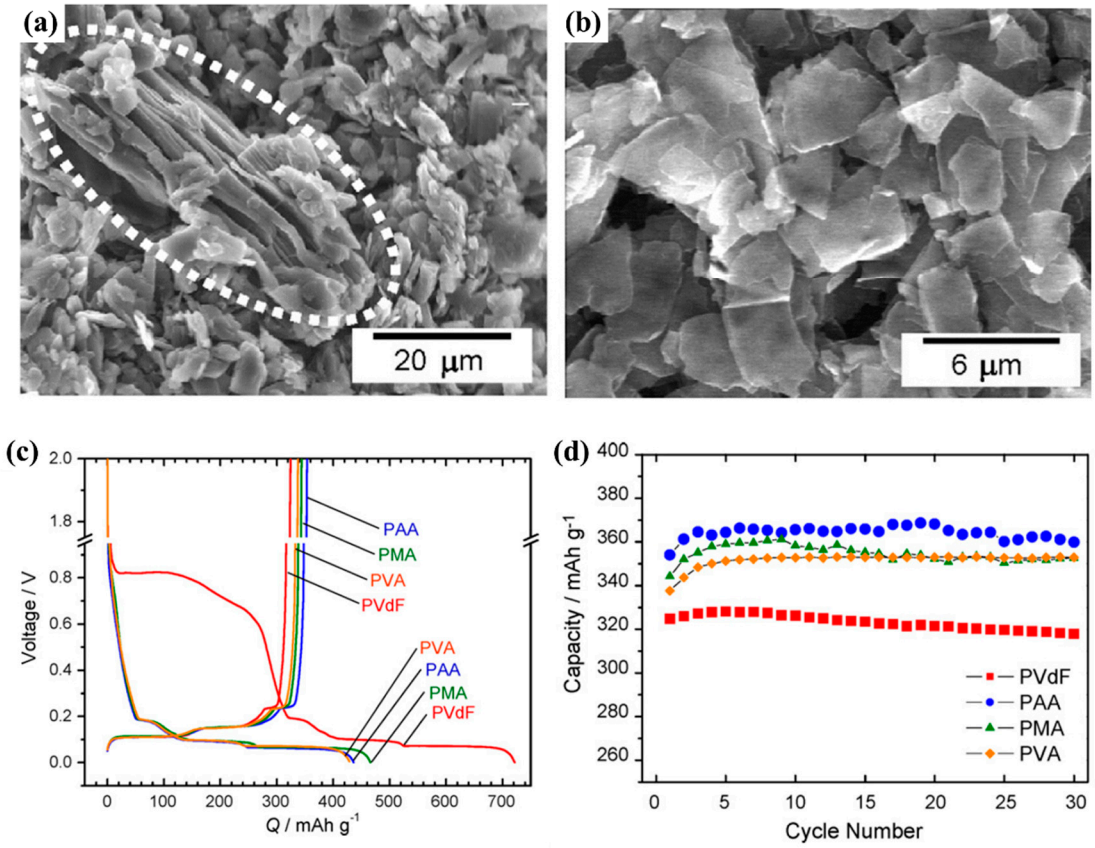

Figure 3. SEM images of Gr electrodes with (**a**) PVDF after the first cycle in $LiClO_4$ in PC. The partial exfoliation of Gr was confirmed. (**b**) PAA after the first cycle in $LiClO_4$ in PC. (**c**) First charge/discharge curves of Gr electrodes with different binders in $LiClO_4$ in PC. The discharge curves have different behaviors for the PVDF electrode, and a noticeable plateau can be seen around 0.8–0.6 V because of enormous co-intercalation causing decomposition of PC molecules, which caused the exfoliation of Gr. (**d**) Cycling stability of Gr electrodes with various binders in $LiClO_4$ in PC electrolyte. The weight % of polymers in the electrodes: PVDF (10%), PAA (15%), PMA (15%), or PVA (5%) in N-Methyl-2-pyrrolidone (NMP). Charge/discharge cycles of the Gr electrode at 50 mA g^{-1} between 0.0 and 2.0 V vs. Li/Li^+ at 25 °C. Reproduced from Ref. [9] with permission from Elsevier.

The Wu group [17] has developed an artificial SEI (A-SEI) on the surface of natural Gr (NG) and artificial Gr (AG) particles via the design of a multifunctional polymer coating to achieve promising electrolyte/A-SEI/electrode interfacial properties. The coated NG electrode demonstrated a capacity of 336 mAh g^{-1}. It showed 95% of full capacity even at a 10 C rate, which was one of the highest rate capabilities reported for an NG electrode. The A-SEI was designed via binary polymeric coating (P&P), including polyallylamine (PAAm) and polyethylene glycol tert-octylphenyl Ether (PEGPE). The achievement of a robust adhesion on the Gr surface was enabled by $\pi-\pi$ attractive interaction of aromatic rings in the PEGPE structure and NH_2 in PAAm, creating strong hydrogen bridge bonding with O in the PEGPE, and nitrogen electrons of the amin groups were utilized to direct Li^+ ions, resulting in an outstanding rate capability of P&P coating Gr electrodes [17] (Figure 4). In another study [76], this group demonstrated β-phase PVDF coating on Cu and Li substrates in ether-based electrolytes, which effectively mitigated Li dendrite formation. They took advantage of using β-phase PVDF and applied it for coating on the Gr electrodes [12] containing a

Li dendrite suppression under severe lithiation conditions in a typical carbonate-based electrolyte and under Li-plating conditions (either 20% over-lithiation or fast lithiation at up to 10C). The polymer-coated Gr electrodes demonstrated good cycling stability with high Coulombic efficiencies (Figure 5) and also offered a new approach to improving the battery safety of LIBs. The PVDF coated on the Gr anode also reduced the charge-transfer resistance due to over-lithiation [12].

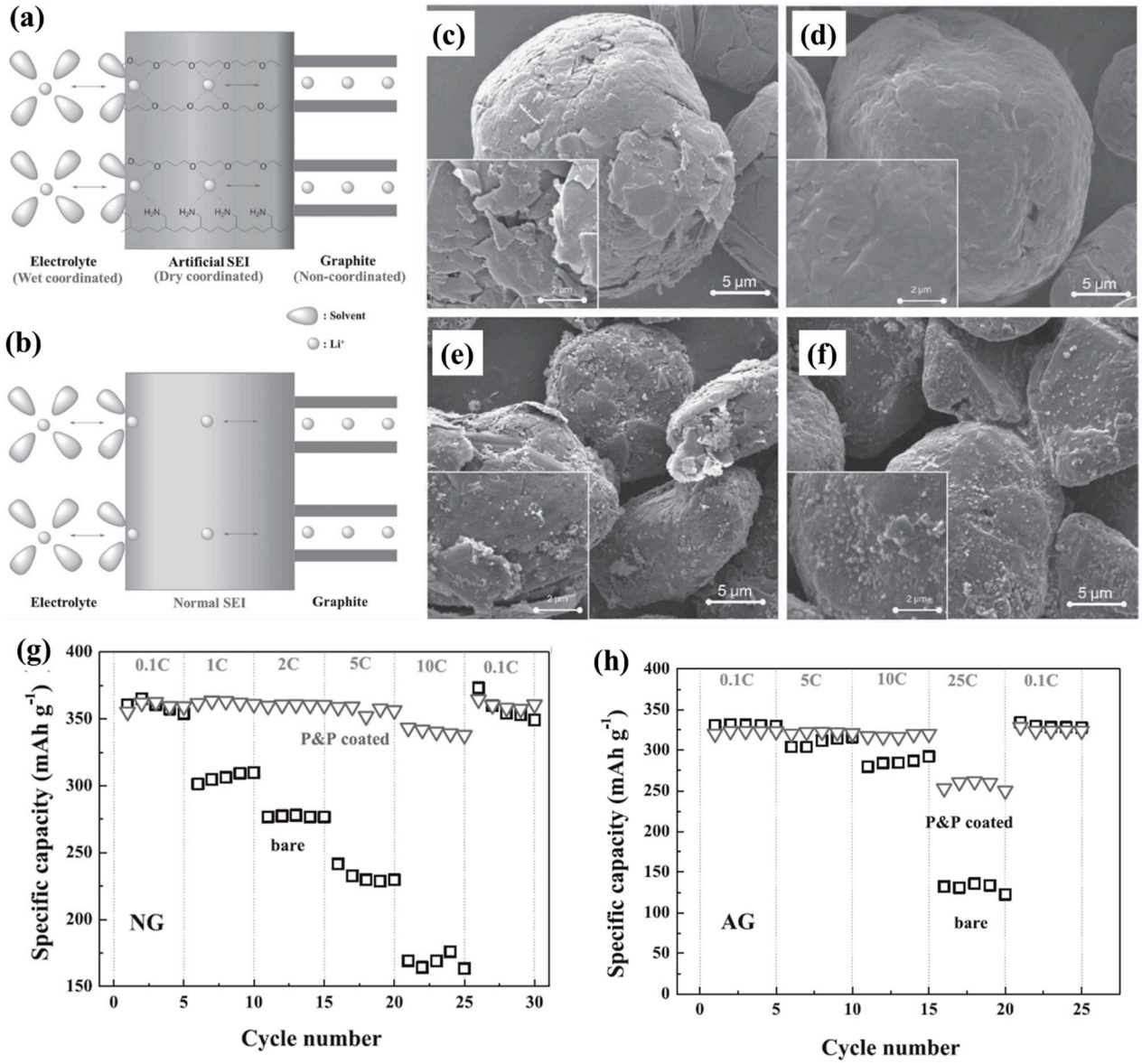

Figure 4. Schematic illustrations of (**a**) the designed A-SEI via binary polymeric coating (P&P) and (**b**) the normal SEI. SEM images of (**c**) bare natural Gr; (**d**) P&P coated natural Gr particles; (**e**) bare Si@Gr particles; (**f**) P&P coated Si@Gr particles. Cycling stability plots at various C-rates for (de)lithiation-specific capacities of (**g**) natural Gr and (**h**) artificial Gr electrodes after lithiation at 0.1 C rate. Gr electrodes: Gr/carbon black (Super-P)/PVDF: 92/3/5 wt%. Electrolyte: 1 M $LiPF_6$ in a mixture of ethylene carbonate (EC), ethyl methyl carbonate (EMC), and dimethyl carbonate (DMC) (1:1:1 in volume) + 1 wt.% vinylene carbonate. 1 C = 372 mA g^{-1}. Reproduced from Ref. [17] with permission from Wiley.

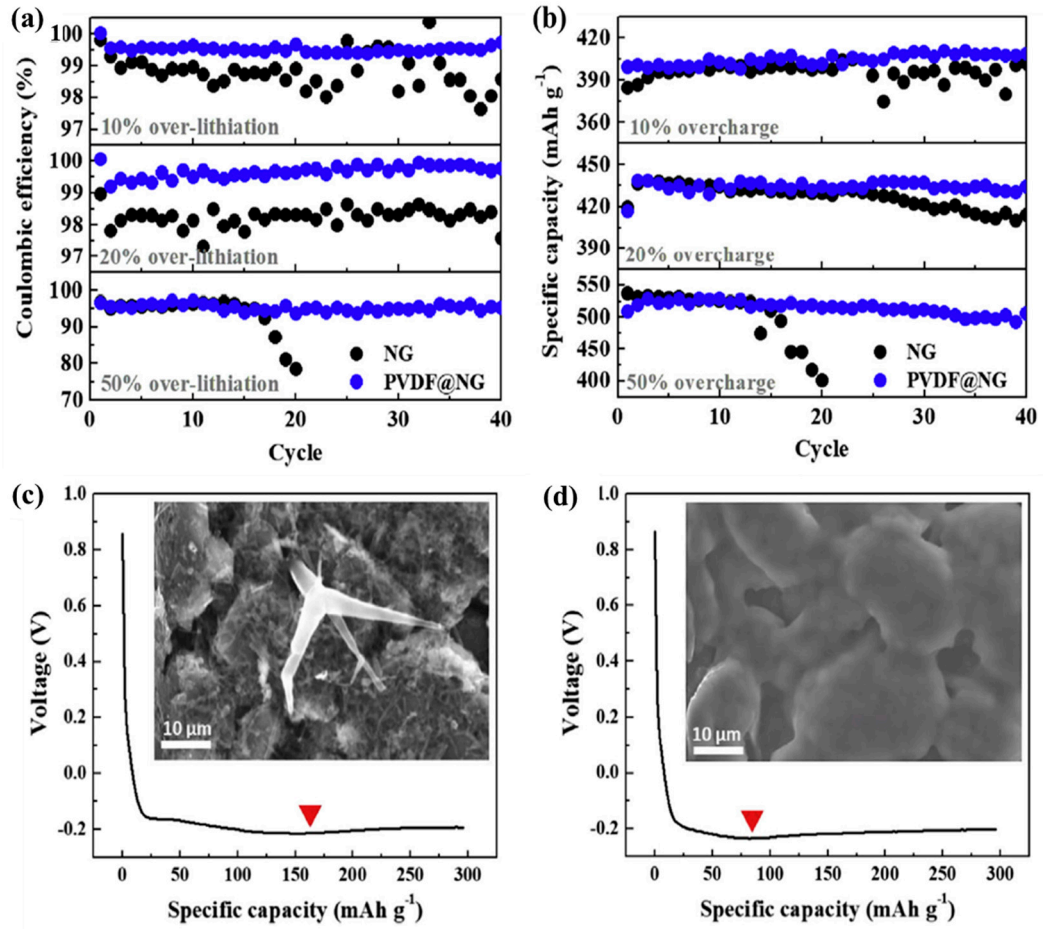

Figure 5. (**a**) CE and (**b**) specific capacity during cycling with various extents of over-lithiation. The coated Gr electrode displayed significantly enhanced cycling stability with high Coulombic efficiencies under the Li-plating conditions. SEM images and corresponding voltage profiles of (**c**) natural Gr electrode and (**d**) PVDF@ natural Gr electrodes under high-rate charging at 10 C for 48 min. Three formation cycles at 0.1 C considering 0.0–1.5 V vs. Li/Li^+. Additional charging for 30, 60, and 150 min at 0.2 C after the cell voltage reached 0.0 V was used to compel over-lithiation cycling, corresponding to 10%, 20%, and 50% of theoretical capacity, respectively. Electrolyte: 1 M $LiPF_6$ in a 1:2 (v/v) mixture of EC/EMC) with 2 wt.% vinylene carbonate (VC) additive. 1 C = 372 mA g^{-1}. Reproduced from Ref. [12] with permission from Elsevier.

Initiated chemical vapor deposition (iCVD) is a low-energy thin film processing tool without using any solvent, which produces thin polymeric films by directly converting one or more monomer vapors to a polymer film on a substrate [77,78]. Thin polymer layers of 1,3,5-trivinyl-1,3,5-trimethylcyclotrisiloxane (V3D3) were coated on the surfaces of Gr electrodes via iCVD [13]. Due to a more steady interface between the active Gr surface and liquid electrolyte and lower charge-transfer resistance, the poly(V3D3) coated Gr electrodes with a coating thickness of about 40 nm acted as a uniform SEI layer consisting of desirable Li-containing compounds, showing higher cycling stability and CE and remaining more steady than the uncoated electrodes. Recently, Seo et al. [39] developed and optimized the thickness of coated PDA on the surface of Gr particles using a wet-based coating method to form a uniform PD layer on the Gr particles as an ion-conducting path for Li-ions. The PD-coated Gr particle improved the electrochemical stability of Gr for both the rate capability and cycling life.

3.2. Titanium Oxide Anodes

Titanium-based anode materials include TiO_2, [79] $Li_4Ti_5O_{12}$ (LTO), [80] and $MLi_2Ti_6O_{14}$ (M = 2Na, Sr, Ba, Pb) [81] as a group of alternative materials to the conventional Gr. As their operation potential is above 0.8 V vs. Li^+/Li, there is consequently no issue in having a stable SEI layer on the active particles [81]. Additionally, a significant safety advantage and superior thermal stability compared to the Gr anode make them attractive and interesting anode materials for LIB applications [81]. However, polymer coating on titanium-based particles could improve rate capability. For instance, Yan Liu et al. [31] have developed a synthesis method to coat LTO particles with a layer of PEDOT:PSS with an average thickness of 3 nm, resulting in an amount of about 1 wt.% of the composite particles. The polymer-coated LTO particles efficiently enhanced electrical conductivity, and the fabricated electrodes were more homogeneous, resulting in a better reversible capacity and rate capability than the pristine LTO electrode. The PEDOT:P PSS-coated LTO delivered a reversible capacity of about 177 and 161 mAh g^{-1} at 0.1 C and 10 C. Nevertheless, LTO particles coated with conductive PTh [33] via an in situ oxidative polymerization method demonstrated a reversible discharge capacity of 172 and 151 mAh g^{-1} at 0.1C and 10C. By adding nitrogen-doped graphene nanosheets to the LTO coated with 10 wt.% PPy anode composites, capacities of about 186 and 152 mAh g^{-1} at 0.1C and 10C were delivered [48]. Slightly lower capacity was achieved for PTh and PPy coated LTO composite anodes compared to the PEDOT:PSS due to the larger amount of PTh or PPy (about 10 wt.% and thickness of 10 to 12 nm) in the composite. Generally, the excellent rate performances for the polymer-coated LTO anodes could be attributed to the conductivity of polymers, which can facilitate the electron and Li^+ transmission during the charge/discharge process tests.

Regarding TiO_2 as an anode material of LIBs, many studies have been conducted [82]. However, coating TiO_2 particles with conductive polymers improved the electrochemical performance of mesoporous TiO_2 [83] and TiO_2 nanoparticles [84] by adding 8 wt.% and 15 wt.% PANi in the composites, respectively.

4. Alloy Anodes

4.1. Silicon-Based Anodes

Silicon (Si), as a low-cost and abundant material, has been considered one of the most studied and attractive anode materials in the pure [10,45,85–88], oxide [89], and composite [71] form for LIBs due to its high gravimetric (4200 mAh g^{-1}) and volumetric capacities (2400 mAh cm^{-3}). However, the diffusion coefficient of Li in Si is low (about 10^{-13} cm^2 s^{-1}) [90], and Si has a low electrical conductivity (10^{-3} S cm^{-1}, which can be increased to about 10^{-2} S cm^{-1} after alloying with Li) [91]. These drawbacks can be solved by adding conductive carbon additives. However, fast capacity fading and high volume expansion, about 300%, during the charge/discharge processes seriously hinder the application of Si anode materials. Until now, several efforts have been focused to solve the mentioned challenges. For instance, some effective methods to solve these challenges include producing Si nanostructures [92,93] and Si/Carbon nanocomposites [71,94,95]. Nevertheless, as an important cause of the failure of Si anodes, the formation of a stable SEI on the surface of Si cannot be achieved with the mentioned methods. Hence, surface modification with a polymer coating on the Si-based anodes is one of the attempts to control SEI formation, which is discussed in the following paragraphs.

PPy, PANi, and PTh have been applied as effective coating layers on Si particles because of their high electrical conductivity, flexibility, and environmental friendliness [44,91,96]. Since PPy can form a conductive matrix, it has been used as a conductive binder and also as an active material in battery and supercapacitor applications [97–101]. Additionally, it acts as a host matrix to avoid significant volumetric expansions during the charge/discharge processes. PPy has been used for coating Si particles with different structures [44,45,86,102,103]. Herein, the important findings will be addressed. Du et al. [44] have studied PPy coating on porous Si hollow nano-spheres via in situ chemical polymerization. The PPy coating significantly enhanced the surface electronic conductivity of Si with excellent structural

stability. Having porous channels in this nanocomposite buffered large volume changes. Additionally, it facilitated the diffusion of electrolyte and Li^+ into the electrode, resulting in a high capacity (1772 mAh g^{-1}) and cycling stability (88% capacity retention after 250 cycles) and a high rate capability (Figure 6). Luo et al. [45] have studied thin PPy coating (thickness of about 6 nm) on Si nanoparticles (NPs) and found that the PPy-coated particle electrodes increased the critical size of Si NPs from 150 nm to about 380 nm.

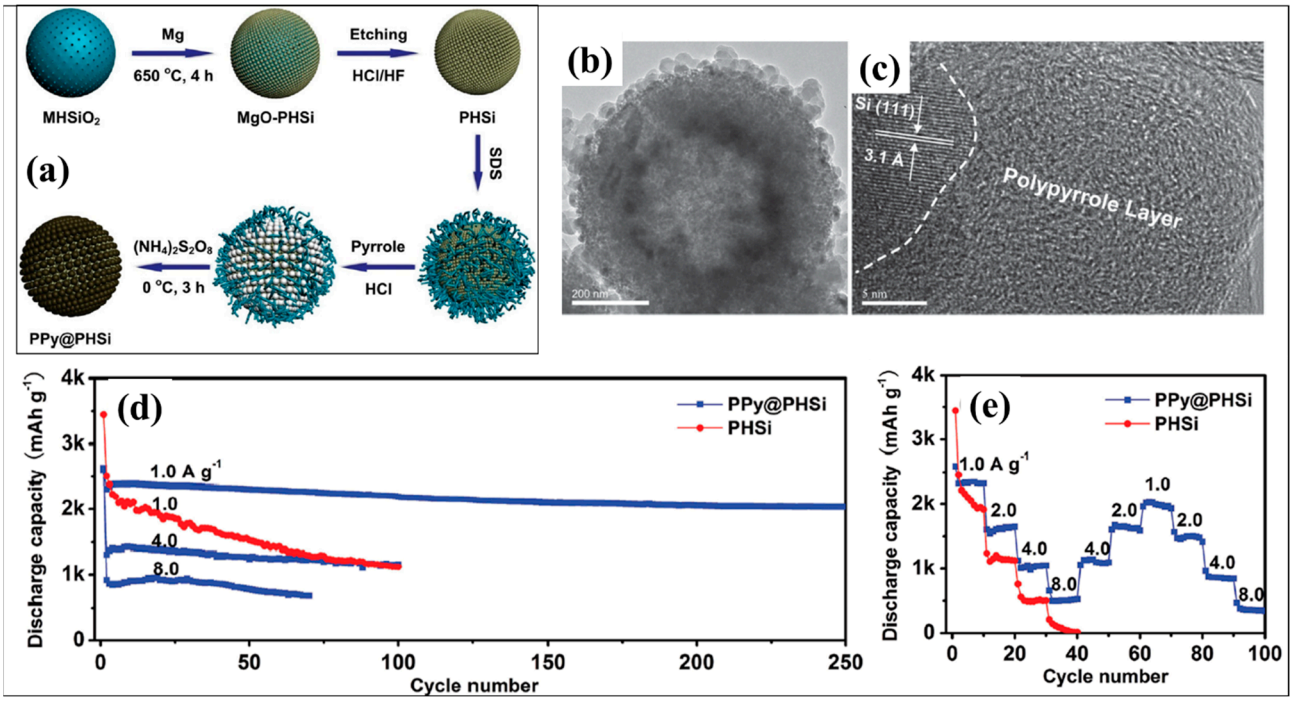

Figure 6. (**a**) Schematic illustration of the fabrication of Si hollow nano-spheres and PPy coating on particles. (**b**,**c**) Microscopic images of polymer-coated samples. (**d**,**e**) Electrochemical characterizations of uncoated and coated electrodes. Reproduced from Ref. [44] with permission from Wiley.

The Bao group [10] demonstrated an interesting synthetic self-healing polymer coated on low-cost Si micro-meter particles, about 3–8 µm. The mechanical damages and cracks of the coated polymers due to the volume expansion of Si particles during the charge/discharge processes could be repaired naturally via the branched hydrogen bonding of the coated polymer, enhancing the Si lifetime anode electrodes with particle sizes in micro-meters. They increased the conductivity of the coated polymers to about 0.25 S cm^1 by adding uniformly conductive carbon nanoparticles into the polymer. CE is critical for the commercialization of every electrode material; the self-healing polymer coating electrode shows an initial CE of about 80%, which is comparable with those electrodes prepared with Si nanoparticles [104–106].

PANi is also an important polymer for coating Si particles [87,96] due to its high conductivity (16 S m^{-1}) [107]. Wu et al. [96] have developed in situ polymerization coating with conductive polymer hydrogel, PANi, placed into Si-based anode electrodes, creating a three-dimensional connection network between the Si nanoparticles and PANi. Additionally, the stable SEI formation on the electrode materials was the reason for the high CE in the half-cell battery tests. The partial carbonization of PANi to carbon on Si nanoparticles was studied by Mu et al. [108]. They obtained a Si/PANi/C composite, which demonstrated better electrochemical performance; although the CE after three cycles reached 99%, the initial CE was about 60%, which is a drawback of this composite. The PANi/$LiClO_4$ film was used for coating on Si@Carbon composite (with a capacity of about 700–800 mAh g^{-1}) materials by the Takeda group [40]. This coating increased the electronic contact of the Si@Carbon composite, held good mechanical integrity, and tolerated the micro-structural change from Si upon the cycling tests, resulting in a stable cycling life compared to uncoated composites.

Pan et al. [109] recently used PANi to coat Si nanoparticles. This composite exhibited a reversible capacity of 1000 mAh g^{-1} at 1 A g^{-1} after 300 cycles, also showing good cycling stability at an areal capacity of 3 mAh cm^{-2} after 150 cycles and an excellent rate performance of 942 mAh g^{-1} at 5 A g^{-1}. Zheng et al. [91] have developed PTh coating on porous Si particles by a simple chemical oxidative polymerization approach. PTh represented a flexible layer to hold Si particles during volume expansion/shrinkage processes and decreased the SEI layer. The Si@PTh composite electrodes demonstrate a longer cycle life with a reversible capacity of 1130.5 mAh g^{-1} at 1 A g^{-1} after 500 cycles. The reason could be an excellent structural stability of the composites and the use of porous Si in the electrodes; however, the main drawback of using porous Si would be low volumetric capacity.

Attia et al. [49] have used a self-assembling polyvinylpyrrolidone (PVP) and polyacrylonitrile (PAN) mixture on the surface of Si NPs, followed by a slow heat treatment process. A robust SiO_2 shell was produced around the Si nanoparticles because PAN improved the oxidation of Si. In contrast, the decomposition of PAN produced a nitrogen-rich carbon coating on the SiO_2 layer, leading to enhanced stability and reversibility of the electrodes. The thickness of the mixed polymers/SiO_2/nitrogen-rich carbon layer was about 3–4 nm. Further improvements were achieved by combining graphene as a conductive network with these particles to produce electrodes with higher stability and electrochemical performance. Using PAN coating also improved Si nanoparticle capacity and cycling life, as shown by Yoon et al. [110]; the composites delivered a specific capacity of 2000 mAh g^{-1}, with a capacity retention of 95% and 75% after 100 and 1000 cycles at 0.5 C, respectively. Fu et al. [50] have developed a coated polyimide on Si NPs by a mechanical stirring process. The polyimide film provided high ionic conductivity and wettability, and the polyimide-coated Si composites revealed much lower Li^+ diffusion resistances than pure Si. However, the polyimide-coated Si anode in the full cell with $LiCoO_2$ as cathode showed poor cycling stability of 50% after only 50 cycles.

A thin, cross-linked polymer film on Si electrodes via iCVD has been studied by Tenhaeff's group using poly(1,3,5,7-tetravinyl-1,3,5,7-tetramethylcyclotetrasiloxane) (pV4D4) as the polymer [51]. pV4D4 films with a thickness of about 25 nm on Si electrodes improved the initial CE and capacity retention over 100 cycles and demonstrated higher rate capability than uncoated electrodes. However, even after 100 cycles, the CE of the coated electrode was low (about 94%), making it difficult for practical application. Using high-energy ball-milling, Si/poly(vinyl alcohol) (PVA) composite particles with a size of about 200 nm were achieved from PVA and micron-sized Si particles [52]. A high initial CE of about 86% and a capacity of 1526 mAh g^{-1} after 100 cycles were obtained with 5 wt.% PVA in the Si composite anodes. The better electrochemical performance could be attributed to using ball-milling. At the same time, the polymer coating effectively reduced the size of Si particles and kept them in nanometer size, thereby shortening the diffusion pathway of Li^+. By applying both polyethylene glycol tert–octylphenyl ether and polymer polyallyl amine (this was explained in the section on graphite), the Wu group [17] succeeded in increasing the capacity of Si from 240 mAh g^{-1} (for uncoated Si electrode) by six-fold to 1630 mAh g^{-1} at 2 C. Although they obtained interesting results, the drawback of this work could be the costly polymers for practical applications.

Recently, Wang et al. [111] synthesized a Si/carbon composite by ball-milling using a waste Si slag, and they used poly(hexaazatrinaphthalene) (PHATN) for coating on Si/carbon composites. The benzene rings in the PHATN could be the active centers for accepting Li-ions, forming stable Li-rich PHATN thin and influential SEI films, which change the LiF's formation path, thereby reducing the consuming electrolytes. Additionally, PHATN molecules expand owing to the change of molecular configuration, providing more space for the volume changes of the Si particles during (de)lithiation processes. This composite anode demonstrated a specific capacity of about 1120 and 417 mAh g^{-1} after 500 cycles at 1.0 and 16.5 A g^{-1}, respectively. PDA coating on SiO_x developed by Gu et al. [112] showed better wetting properties with water and electrolyte solution. It delivered an initial Columbic efficiency of 80.48% and excellent specific capacities of about

1270 and 1140 mAh g^{-1} at 0.05 and 3 C, respectively, and a capacity retention of about 80% after 150 cycles at 1 C.

4.2. Silicon@Graphite (Si@Gr)

Wu's group [58] has developed a mixed polymer, including poly(diallyl dimethylammonium chloride) and poly(sodium 4-styrenesulfonate) (PDDA–PSS polymer) on the surface of Si/Gr composite materials containing Si NPs. They showed that the PDDA–PSS polymer, in addition to surface coating, also improved the uniformity of Si NPs distribution on the Gr surface and maintained the Si particles during volume changes without separation, thus allowing the NPs to maintain close contact with Gr micro-particles. The coated electrodes demonstrated higher Coulombic efficiencies throughout the cycling, a specific capacity of 450 mAh g^{-1} at a lower C-rate, with 95% retention after 200 cycles, and an outstanding rate capability of 96% capacity retention (426 mAh g^{-1}) at 10 C. However, the uncoated Si/Gr electrode presented poor performance, less than 200 mAh g^{-1} at 10 C. Furthermore, the PDDA–PSS-coated Si/Gr exhibited the same volume expansion as the pristine Gr electrode. Kim et al. [57] investigated poly(vinyl alcohol)-PO_4 (PVA-PO_4) coating on Si/Gr composites. Si/Gr materials were prepared by ball-milling with 30% Si in the composite, and the PVA$-PO_4$ on the surface of Si/Gr was produced again by ball-milling of PVA, $NH_4H_2PO_4$, and Si/Gr particles. Electrochemical improvements were pronounced for the PVA-PO_4 coated Si/Gr composites and delivered a discharge capacity of about 1500 mAh g^{-1}, and stable CE throughout the cycles thus provided a particular improvement. Here, the PVA–PO_4 acted as a binder in addition to lithium polyacrylate, reducing the electrode's pulverization. Furthermore, it preserved stable Li_2O with high ionic conductivity during cycling, forming a stable SEI layer.

Recently, Abdollahifar et al. [38] developed a chitosan coating on Si/Gr particles as an artificial SEI layer using a simple solution method. The coating was made of sulfonated chitosan and cross-linked with glutaraldehyde, promoting good ionic conduction and sufficient mechanical strength of the polymer layer. The coated Si/Gr composite anodes demonstrated a capacity of 600 mAh g^{-1}, with excellent cycling stability of up to 1000 cycles. The coated polymer improved CE by reducing active Li losses and electrolyte consumption. A significantly enhanced cycling stability of the chitosan-coated anodes could be ascribed to the artificial SEI function of the polymer coating. It exhibited a cation (Li^+)-selective behavior to facilitate the diffusion of Li-ions between the electrolytes and the Si/Gr composite material.

4.3. Tin (Sn)-Based Anodes

Several high-capacity anode materials have been reported and studied widely as promising candidates for LIBs applications, such as Tin (Sn), Si, metal oxides, and Li metal, due to their high theoretical capacity and natural abundance. High electrical conductivity of Sn, make it an attractive anode condidate for LIB applications. However, this material experiences low initial CE, which could be avoided using a Li_xSn alloy, which also serves as a potent Li-containing anode material [113,114]. Li_xSn alloys have gained much attention due to the high theoretical specific capacity of $Li_{4.4}Sn$, which equals 788 mAh g^{-1} [113,115]. Like Si anodes, Sn also has a major drawback due to its significant volume changes during cycling, which can cause severe mechanical damage to the anode, eventually leading to capacity fading of the cell, and gradual aggregation of Li_xSn/Sn. Some of the efforts that have been introduced to solve the above issues include nanosizing the active material and introducing porosity into the structure, as well as the surface coating [113,116,117]. Surface polymer coating is an exciting method for protecting the micro-structure of the electrode that experiences internal stress while protecting the surface of the active material from side reactions. Nevertheless, the role of surface polymer coating in the particle networks of anodes remains challenging. The following section will discuss polymer coating on Sn-based anode materials.

Fan et al. [118] reported that the ultra-thin 3D PPy coating (3–4 nm) generated in situ on the surface of Sn nanoparticles provided structural integrity and increased capacity. The

3D-PPy-coated Sn anodes result in a higher specific capacity of 766 mAh g^{-1} (0.2 A g^{-1}) and 583 mAh g^{-1} (2 A g^{-1}). It was shown that the conductive polymer had multiple functions and acted as a binder and a conductive network in which the Sn nanoparticles are dispersed. The reference electrodes without a 3D conductive network demonstrated a capacity of 375 mAh g^{-1} after similar cycles. In a study accomplished by Li et al. [119], the various thicknesses (8–40 nm) of PPy coating on Sn nanoparticles were used as protection during the lithiation step. The optimized coating thickness of 20 nm stabilized the Li_xSn nanoparticles (Li_xSn@PPy), and this composite anode showed an excellent specific capacity of 534 mAh g^{-1} after 300 cycles, with a capacity retention of 86%. Moreover, the optimized PPy coating offers less volume expansion of the active anode material and prevents the agglomeration of Li_xSn particles. It is claimed that the PPy conductive polymer coating provides the channels of fast electron diffusion and enables quicker reaction kinetics. Cao et al. reported on the PEO-coated Sn anodes, where the polymer should act as a passivation layer that neutralizes the volume expansion of the active material during cycling [120].

4.4. SnO_2

One of the most promising candidates for anode materials among the metal oxides is SnO_2 owing to the high theoretical capacity, safe working potential, and natural abundance. The oxide of Sn also suffers from significant volume change (>300%) during cycling [117]. The electrochemical reactions of Li and SnO_2 can be seen below Equations (1) and (2). Assuming that the reactions are fully irreversible, a reversible theoretical capacity of 782 and 1494 mAh g^{-1} can be obtained.

$$SnO_2 + 4Li^+ + 4e^- \rightarrow Sn + 2Li_2O \quad (1)$$

$$Sn + xLi^+ + xe^- \rightarrow Li_xSn\ (0 \leq x \leq 4.4) \quad (2)$$

Yuan et al. reported on the SnO_2-PPy composite anodes through the chemical polymerization method [26]. The SnO_2-PPy (18.25% of SnO_2 amount of loading) composite anode and bare SnO_2 anode delivered a discharge capacity of 562 (1st cycle) and 450 mAh g^{-1} (20th cycle), and 570 (1st cycle) and 250 mAh g^{-1} (20th cycle), respectively. The proposed mechanism for improved cycling stability of the SnO_2-PPy composite anode is that the concentration of polymer PPy acts as a conductive matrix and buffers the volume change reductions in the active composite anode material, resulting in Li_xSn alloying and de-alloying reactions. Cui L et al. reported on one-dimensional (1D) nanocomposites of 79 wt.% of SnO_2@PPy, which exhibit a capacity of 430 mAh g^{-1} after 20 cycles, which is three times higher than bare SnO_2 [121]. Shao Q.-G et al. designed SnO_2 with a multi-walled carbon nanotube (MWCNT) and as a protective layer of the surface coating of PPy (SnO_2@MWCNT@SnO_2@PPy). The composite anode materials with higher conductivity effectively suppressed mechanical stress and prevented the aggregation of SnO_2 nanoparticles, delivering 600 mAh g^{-1} for 30 cycles [27].

Liu et al. prepared the core-shell hollow SnO_2@PPy with the hydrothermal method, after which the in situ chemical polymerization took place [28]. The nanocomposites of SnO_2@PPy (21 wt%) result in a specific capacity of 1036 and 331 mAh g^{-1} at the current density of 0.1C and 2.0C, respectively. The polymer coating prevents the pulverization of the hollow SnO_2 and prevents them from aggregating. Zhou M et al. reported on the double-shelled hollow micro-spheres with poly(ethyleneglycol dimethacrylate-co-methacrylic acid as SnO_2/P(EGDMA-co-MAA)composite anodes, which showed a high capacity retention of 49.5 wt%. The initial discharge and charge capacity of SnO_2/P(EGDMA-co-MAA) with 35.3 wt.% SnO_2 (18 nm) and 49.5 wt.% SnO_2 (24 nm) showed a capacity of 1170, 896, 689, and 470 mAh g^{-1}, respectively [122]. After 430 cycles, the SnO_2/P(EGDMA-co-MAA) composite anode displayed a discharge capacity of 711 mAh g^{-1}. Cao et al. reported that the PPy polymer coating played an interesting role in SnO_2 nanoparticles (SnO_2@PPy) and resulted in an initial discharge/charge of 935 and 723 mA h g^{-1} with a CE of 77%. The effects

between the PPy-coated SnO_2 and the hollow structure can decrease the pulverization of SnO_2 [29].

Li et al. have used the in situ transmission electron microscopy (TEM) to study the role of interparticle connections in SnO_2 nanoparticles with different coating layers of PPy and metal oxide MnO_2 [123]. The PPy coating layers in SnO_2@PPy provide a large contact area and robust adhesion between SnO_2 nanoparticles, demonstrating a better cycling stability and fast kinetics. The SnO_2 NPs@MnO_2 layer showed a specific capacity of 680 mAh g^{-1} after 10 cycles. However, SnO_2@PPy (20 nm) delivered a stable capacity of 780 mA h g^{-1} with a current rate of 0.1 C over 400 cycles. Recently, Zhang et al. [37] studied the PPy polymer coating on SnO_2 nanoparticles coated with the sol–gel method. The SnO_2 encapsulated by the conductive PPy showed specific capacities of 930 and 560 mAh g^{-1} at 0.2 and 2 A g^{-1}, respectively. Li et al. introduced the hierarchical SnO_2 spheres coated with PPy, which improved conductivity and accommodated the structural integrity during cycling [124]. This composite anode resulted in a stable cyclability of 782 mAh g^{-1} (at 0.25 C) after 650 cycles and 580 mAh g^{-1} (at 4.0 C) after 5000 cycles.

Arif et al. reported a ternary-type SnO_2 nanocomposite as an anode incorporated with reduced graphene oxide (rGO) and PEDOT:PSS as a conductive polymer [125]. This work reports that 5 wt.% of PEDOT:PSS coated on the SnO_2/rGO composite delivers an improved capacity of 980 mAh g^{-1} (0.1 C) with a CE over 99% after 160 cycles; both the rGO and the PEDOT:PSS act as the conductive medium and buffer the volume change of SnO_2 NPs. The PDA-coated SnO_2 [117] with a layer thickness of 5 nm exhibited significantly improved cycling stability and demonstrated good cyclability for over 300 cycles. Li et al. reported a facile approach combined with hydrothermal treatment and polymerization to fabricate the core-shell-structured SnO_2@C/PEDOT:PSS micro-sphere anodes, as seen in Figure 7a [126]. For a better understanding of structural changes during cycling, the TEM images of the SnO_2@C anode after 200 cycles at a current rate of 0.5 C are depicted in Figure 7b,c. The TEM images show a stable micro-sphere morphology that helps avoid aggregation during the cycling process. However, without polymer coating, the bare anode materials exhibited cracks and fractures, leading to an unstable structure and degrading the electrochemical performance. The group reported the initial specific capacity of 1170 mAh g^{-1} at a current rate of 0.1 C and 441 mAh g^{-1} for 1200 cycles at a high current rate of 2C (Figure 7d). The PEDOT:PSS polymer coating accommodates the volumetric change of SnO_2. Guo et al. reported that the in situ polymerization of SnO_2-Fe_2O_3@PANi results in anodes with an excellent capacity of 1000 mAh g^{-1} (current density of 400 mA g^1) after 380 cycles [127]. Adding a carbon layer can improve the electronic conductivity of the anode, and in situ polymerization of PANi coating prevents agglomeration and particle growth during the heat treatment. This method ensures homogeneous carbon coating, thus providing good conductive contact between SnO_2-Fe_2O_3 and the carbon shield surrounded by the anode. Table 2 summarizes the effect of polymer coating on the performance of some reported SnO_2 anodes.

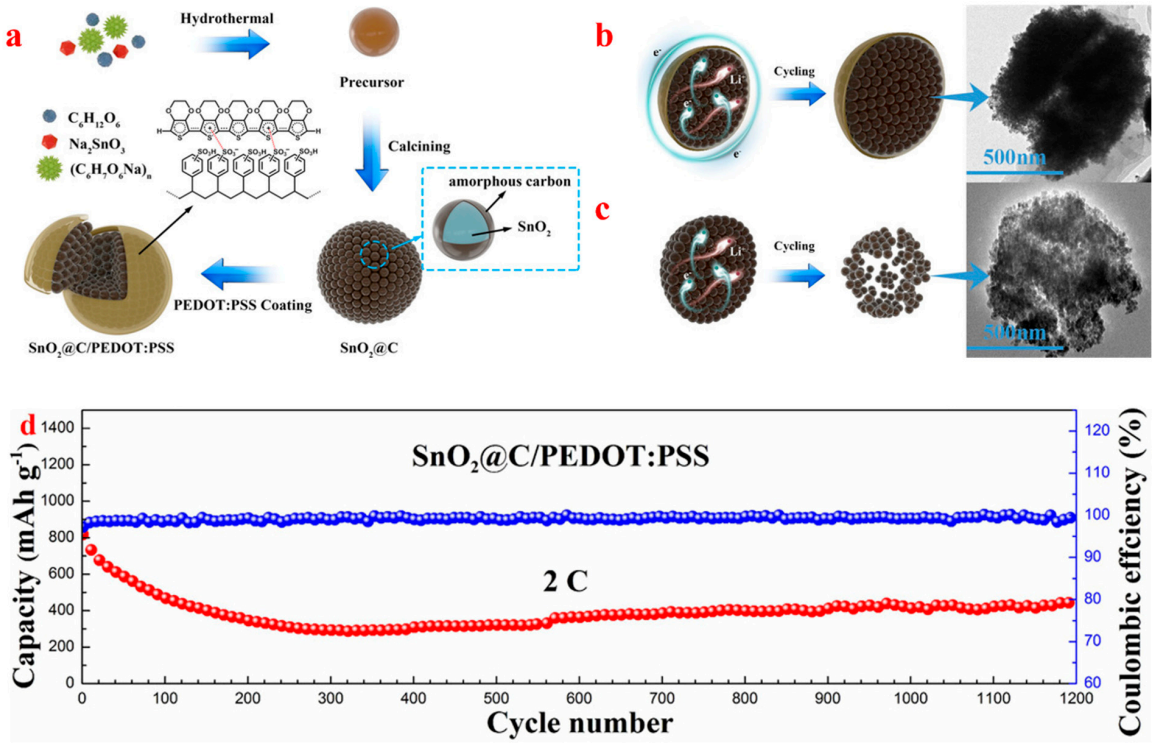

Figure 7. (**a**) The hydrothermal synthesis of PEDOT:PSS coated SnO_2@C anodes. (**b**,**c**) TEM morphology of SnO_2@C/PEDOT:PSS and bare SnO_2@C after the cycling performance. (**d**) The SnO_2@C/PEDOT: PSS composite anode cycling performances with rate cyclability at 2 C and CE. Reproduced from Ref. [126] with permission from Wiley.

Table 2. Various polymer coatings applied to SnO_2-based anodes and their electrochemical performances.

Polymer	Synthesis Method	Coating on Particle/Electrode	Thickness	Cycling Performance (mAh g^{-1})/Current Rate (mA g^{-1})	Ref.
Polypyrrole (PPy)	Chemical polymerization method	Electrode	-	450 (20 cycles)/50 250 (20 cycles for bare SnO_2)/50	[26]
	Chemical polymerization method	Particle	-	600 (30 cycles)/100	[27]
	In situ chemical polymerization	Electrode	-	430 (20 cycles)/50	[121]
	Hydrothermal method and in situ chemical-polymerization	Particle	25 nm	448.4 (100 cycles)/78	[28]
	Chemical vapor-phase polymerization	Electrode	20 nm	646 (150 cycles)/100	[29]
	In situ coating method	Particle	20 nm	760 (400 cycles)/0.1 C	[123]
Poly(3,4-ethylenedioxythiophene-poly(styrenesulfonate) (PEDOT:PSS)	Wet chemical method	Particle	2–3 nm	980 (160 cycles)/80	[125]
	Hydrothermal method and polymerization	Particle	6 nm	441.5 (1200 cycles)/2 C	[126]
Poly(ethyleneglycol dimethacrylate-co-methacrylic acid)	Hydrothermal method and polymerization	Particle	24.5 nm	711.9 (430 cycles)/200	[122]
Polydopamine (PDA)	Wet chemical method	Electrode	5 nm	1502 (300 cycles)/160	[117]

4.5. Other Tin (Sn)-Based Anodes

Sn−Ni-alloy-type anode materials are promising candidates for LIBs, with a simple fabrication method, higher capacity, and conductivities. Sn-Ni nanotubes have boosted mechanical strength and efficient electron transfer in the nanotube, but they also partly improved the mechanical stress during Sn volume expansions. A study conducted by Fan et al. used PEO to control the formation of SEI and stabilize the anode structure despite the volume changes, as well as to stabilize the electrode interface [128]. It was shown that adding a thin PEO coating to the Sn−Ni alloy nanotubes improves the cycling and rate performance. How-

ever, the 1D nanotube morphology may not be optimal for battery applications, and a three-dimensional (3D) configuration could be more beneficial due to the larger active surface area of the electrodes. Gowda et al. introduced the conformal coatings of PMMA (25–30 nm), which were deposited on the Sn–Ni alloy anode materials and served as a gel-type electrolyte after being soaked with liquid electrolyte for the application of LIBs (Figure 8) [129]. The 3D Sn−Ni@PEO composite exhibited reversible capacities of 939 and 533 mAh g^{-1} at the current densities of 0.2 and 5 A g^{-1}, respectively [128]. Over 80 cycles, the composite anode retained its specific capacities of 619 and 170 mAh g^{-1}, with current rates of 0.2 and 5 A g^{-1}, respectively (Figure 8). The nanotube array anode Sn/Ni@PEO shows a stable discharge capacity of 806 mAh g^{-1} over 200 cycles. On the other hand, the Sn/Ni nanotube array without the PEO coating resulted in a capacity of 600 mAh g^{-1} after 200 cycles [130]. The composite system Sn/Ni@PEO combines the 3D hollow nanostructure of the active material and the surface coating of PEO for accompanying the volume expansion of Sn, delivering higher cycle stability, better contact with the current collector, and high rate performance. Tolganbek et al. recently introduced a layer-by-layer method (LBL) for coating a thin polymer electrolyte onto 3D Ni_3Sn_4 anode particles (Figure 8). This method has the advantage of controlling the thickness of the deposited polymer layer on the 3D active material structure. Figure 8c represents the Ni_3Sn_4 anode/gel-like polymer electrolyte (GPE)/$LiFePO_4$ cathode 3D cells scheme, fabricated using the LBL deposition method [36]. With this design, the cells showed a capacity of 143 mAh g^{-1} over 100 cycles (Figure 8c,d).

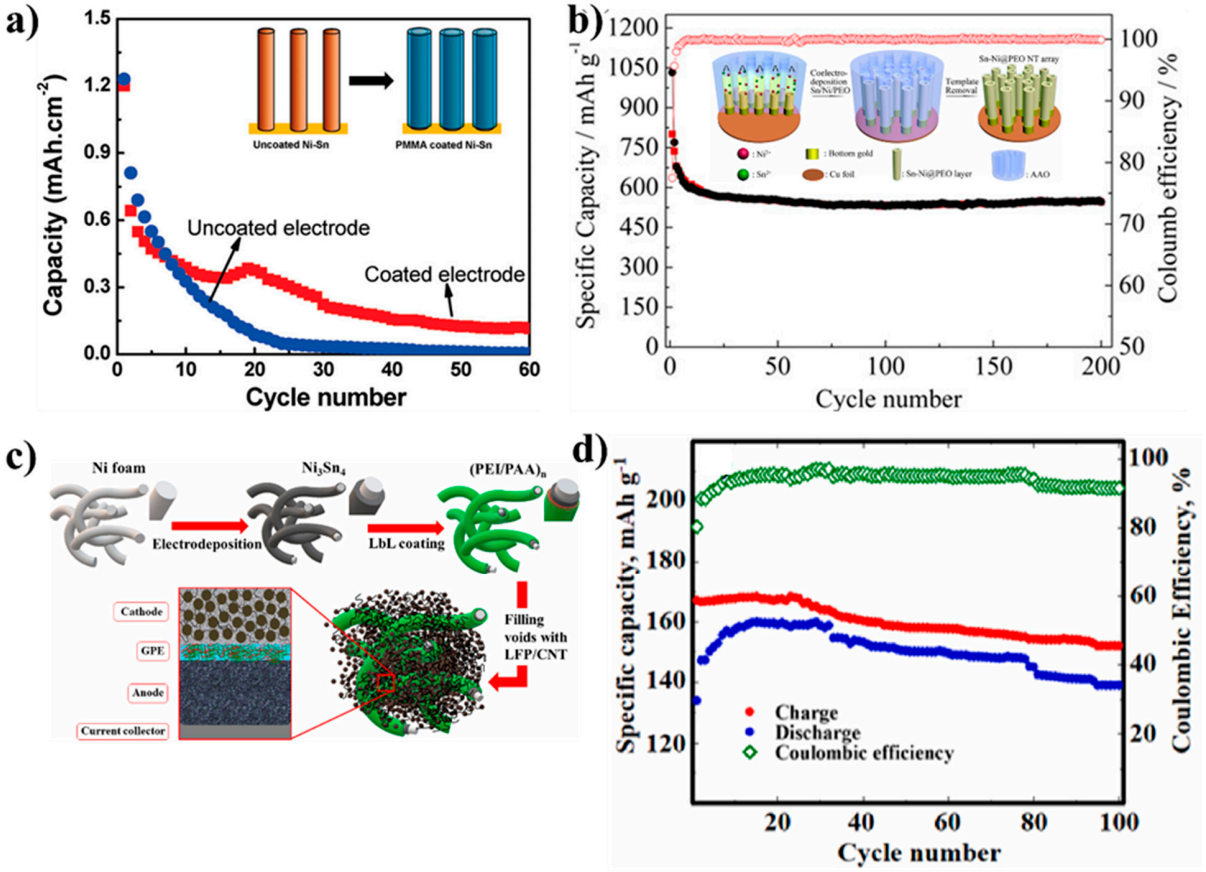

Figure 8. (**a**) The cycling performance of PMMA-polymer-coated Ni−Sn and bare Ni−Sn nanowires. The three-dimensional PMMA-coated Ni−Sn nanowires (in blue color) and the uncoated Ni−Sn nanowires cycled (in red color) at the rate of 0.3 mA cm^{-2} (or 3.0 C). Reproduced from Ref. [130] with permission from the American Chemical Society. (**b**) A schematic representation of the Sn–Ni@PEO nanotube formation. Reproduced from Ref. [128] with permission from the American Chemical Society. (**c**,**d**) A 3D full battery fabrication consists of the Ni_3Sn_4 alloy as an anode material and $LiFePO_4$ (LFP) as a cathode at 0.1 C. Reproduced from Ref. [36] with permission from Elsevier.

4.6. Germanium (Ge)

In terms of Ge, with a theoretical capacity of 1600 mAh g^{-1} and a volumetric capacity of about 8500 mAh cm^3 and with a better electronic conductivity and transmission rate of Li^+ than Si, much attention has been paid to the anodes of LIBs [131,132]. However, Ge displays volume expansion up to 300% during cycling, delivering low initial CE and poor cyclability [133–135]. Polymer coating on the particles [59] and electrodes [32] can be used to improve these issues. Regarding electrode coating, Sun et al. [32] established a method for producing high-performance Ge film electrodes grown on a 3D current collector (CuO) and an in situ formation of PVDF−hexafluoropropene/SiO_2 (PVDF-HFP/SiO_2) protective layer on the electrode surface. The coated polymer improved the mechanical and ionic/electronic transport properties of Ge, which led to high reversible capacity (about 1100 mAh g^{-1}) and cycling stability over 3000 cycles at 1 C rate with 95% retention and an excellent rate capability even at 10 C (974 mAh g^{-1}). Moreover, after a few initial cycles, the electrodes showed a high CE of 99.9%, indicating good reversibility for the (de)lithiation processes. The PEDOT:PSS coating (about 3 wt.%) on the surface of Ge nanoparticles (10–100 nm) was developed by Liu et al. [59]. The PEDOT:PSS coated Ge electrode improved the initial CE from 81% (for the pristine electrode) to 89% and demonstrated an excellent rate performance at 2 C (800 mAh g^{-1}) and 4 C (700 mAh g^{-1}), whereas the uncoated electrode showed almost no capacity at 2 C.

5. Conversion Anodes

Conversion anodes mainly include, but are not limited to, transition metal oxides, sulfides [136], phosphides [137–140], and nitrides [141–144]. Herein, polymer coating on the transition metal oxides will be discussed.

5.1. Iron Oxides

Iron oxide anodes, such as Hematite, α-Fe_2O_3 (paramagnetic mineral only in a Fe^{2+} oxidation state, with a theoretical capacity of 1007 mAh g^{-1}), and Fe_3O_4 (ferromagnetic material in both Fe^{2+} and Fe^{3+} oxidation states, with a theoretical capacity of 926 mAh g^{-1}), are non-toxic, natural abundance, easy-to-prepare, low-cost materials with high electronic conductivity and have been considered as one of the high-capacity anode candidates for LIBs. Except for the higher theoretical capacity and density (5.24 g cm^{-3}), iron oxide anodes could be safer than Gr (2.16 g cm^{-3}) owing to their higher potential, which reduces Li dendrite deposition on the anodes during charge/discharge cycling. However, iron oxide anodes suffer from poor rate capability and long-term cyclability because of the large volume change (over 200%) during Li-ion (de)intercalation (conversion reaction) processes [145–154]. Therefore, many approaches have been proposed to increase the iron-oxide-based anodes' cyclability and rate capacity [155–159]. Polymer coating on the particular structures of iron oxide particles, in a study by Jeong et al. [42], for instance, could provide a unique electrode structure with a short diffusion distance for ions and a fast mass transport channel for the electrolyte and necessary void spaces for significant volume variations during the cycling tests. They prepared a hierarchical core-shell hollow structure of α-Fe_2O_3 coated with PANi as an anode material via in situ polymerization. α-Fe_2O_3@PANi hollow structure anodes delivered efficient and fast ion/electron pathways for electrochemical reactions. Furthermore, more space for significant volume expansions resulted in a large reversible capacity (958 mAh g^{-1} at 0.1 C), high rate capability (793 mAh g^{-1} at 5 C and 724 mAh g^{-1} at 10 C), and better cycling stability (Figure 9). Liu et al. [160] used PPy for coating α-Fe_2O_3 particles directly on the iron foil as a current collector to produce a unique structure. The α-Fe_2O_3@PPy electrodes showed a specific capacity of 0.42 mAh cm^2 at 0.1 mA cm^2; however, no improvement was achieved for the cycling stabilities compared to the uncoated electrodes. To enhance the cycling stability of Fe_2O_3 when PPy is used as a coating polymer, carbon coating on Fe_2O_3 before polymer coating is a critical step, as shown by Han et al. [43]. Due to the use of Fe_2O_3 NPs, a porous carbon matrix, and the formation of two protective layers of carbon and PPy, this unique nanostructure with improved electrical

conductivity demonstrated better electrochemical performance. This composite showed a practical capacity of 1004 mAh g^{-1} with a Fe_2O_3 loading (47 wt.%) close to the theoretical capacity. High volumetric capacity is another advantage of using iron oxide anodes—an essential parameter in cell packs. The volumetric capacity of the Fe_2O_3@Carbon/PPy composite was about 816 mAh cm^{-3}, which is more than two times that of conventional Gr electrodes (about 370 mAh cm^3) [161].

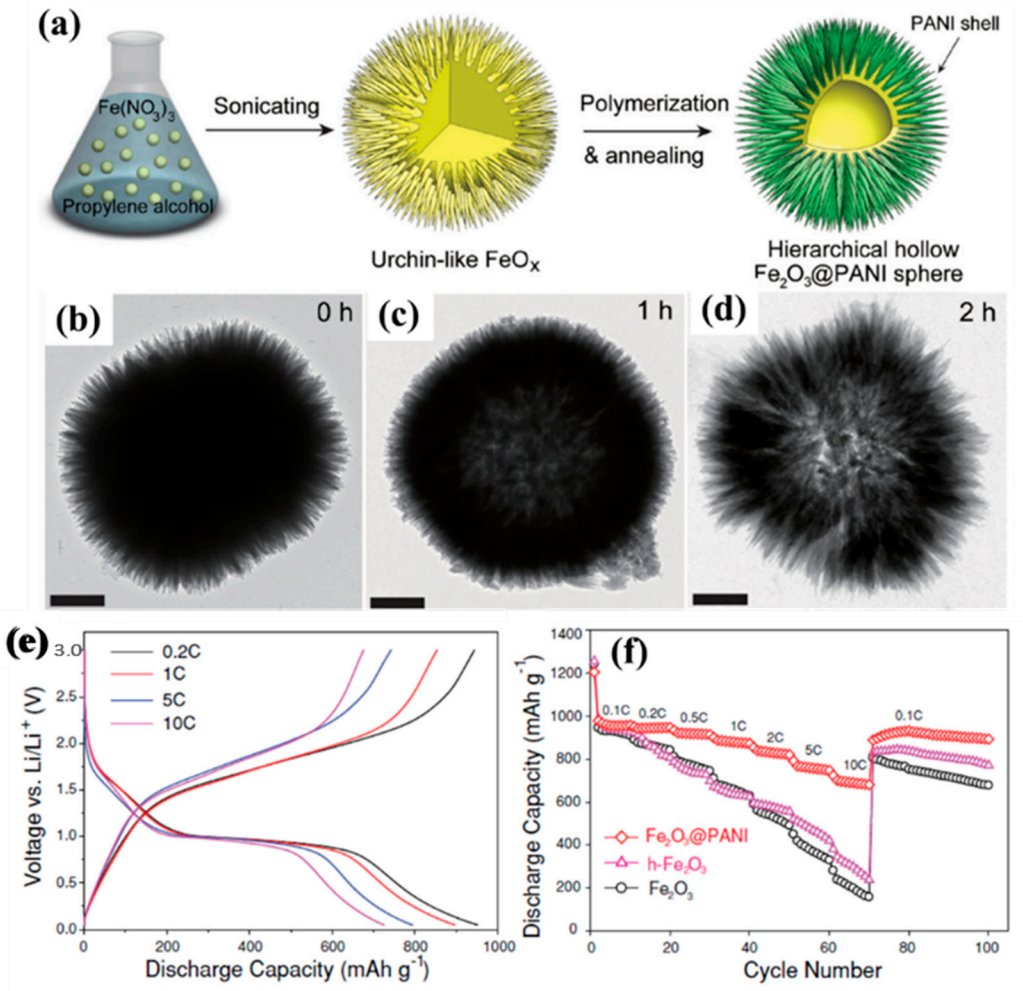

Figure 9. (**a**) Schematic demonstration of the procedure for synthesis of hierarchical Fe_2O_3/PANi. (**b**–**d**) TEM images of the particles were obtained with various reaction times for PANi polymerization (scale bar is 200 nm). (**e**,**f**) Rate performance of Fe_2O_3/PANi electrode at rates 0.1 C–10 C. Reproduced from Ref. [42] with permission from Wiley.

In order to protect Fe_3O_4 from structural variation, prevent the aggregation of NPs, and avoid direct contact between the active materials and the electrolyte, an effective polymer, PPy, was used to coat Fe_3O_4 NPs [162]. The Fe_3O_4@PPy composite demonstrated notable capacity retention of 98% of the initial capacity (544 mAh g^{-1}) after 300 cycles. In this study, the remarkable cycling stability could be due to the high content of PPy (about 40 wt.%) in the composite. Coating Fe_3O_4 hollow nano-sphere particles (about 200 nm) with PANi can also increase the reversible capacity (1090 mAh g^{-1} at 50 mA g^{-1}) and improve its rate capability compared to uncoated and solid particles of Fe_3O_4 [163].

5.2. MnO_2

Although manganese (Mn) oxides are well-known materials for supercapacitor applications [164], they can also be applied as electrode materials for LIBs [165,166] and other types of batteries [167–170]. Among the Mn-oxide materials, MnO_2 received more

attention for LIBs applications due to its low cost, natural abundance, environmental friendliness, low discharge voltage plateau, and, importantly, a high theoretical capacity of 1230 mAh g^{-1}. However, Mn-oxides exhibit low electrical conductivity (10^{-5} to 10^{-6} S cm^{-1}) [171] and significant volume variations during (de)lithiation processes [172]. Additionally, they suffer from Mn dissolution [173–175], leading to degradation of the electrochemical performance in terms of rate capability and cyclic stability. The polymer coating can relatively overcome the drawbacks mentioned above. For instance, Chen et al. [55] synthesized MnO_2 nano-boxes and demonstrated that PEDOT coated on the surface of MnO_2 nano-boxes (edge and shell of about 300 nm and 50 nm) by in situ polymerization of 3,4-ethylenedioxythiophene offers the paths for Li-ion diffusion and the space to buffer the volume variations. The conductive polymer guarantees structural stability and increases the electronic conductivity of MnO_2, resulting in improved electrochemical performances with a reversible capacity of 628 mAh g^{-1} after 850 cycles at 1 A g^{-1}. Xiao et al. [41] studied ultra-thin MnO_2 nanosheets coated with PTh, which improved the capacity and cycling stability and delivered a reversible capacity of 500 mAh g^{-1} after 100 cycles at 500 mA g^{-1}. However, the uncoated electrode only retained a capacity of 250 mAh g^{-1} after the same cycling. PPy could also improve the MnO_2 electrochemical performance, which was shown by Garakani et al. [171]. They used MnO_2 nanowires@PPy core shell grown on graphene foam to increase conductivity and achieve a stable structure against volume expansion upon lithiation. The PPy-coated MnO_2 electrode demonstrated a three-times-faster lithiation speed than the uncoated MnO_2. It showed a reversible capacity of 945 mAh g^{-1} at 0.1 A g^{-1}, while the uncoated electrode only showed 550 mAh g^{-1} after 150 cycles.

5.3. Copper Oxide (CuO)

Copper oxide (CuO), another interesting and low-cost transition metal oxide, has been used as an anode for LIBs [176–179] because of its high theoretical capacity of 674 mAh g^{-1} [178] and environmental benignity. However, this low conductive material shows a significant volume expansion (174%) upon lithiation [180] and low initial CE (35% to 65%) [181–183]. Therefore, these critical issues need to be resolved for practical applications. The PPy coating on CuO particles could minimize the mentioned challenges [34,46,184]. For instance, Yin et al. [46] synthesized various CuO particles with shell nano-belt structures by controlling the polymerization time of pyrrole. The shell played a vital role in Li storage properties of the final composite, along with using sodium dodecyl sulfate (surfactant) as a key factor in obtaining high-value core-shell nanostructures. Within three hours of polymerization, about 7 wt.% PPy was produced on the CuO composite, providing a high reversible capacity of 760 mAh g^{-1} after 45 cycles. They also showed some improvements in another study [184]. Zhou et al. [34] developed an evaporation method for the in situ polymerization of PPy on CuO arrays for uniform polymer coatings. The uniform polymer coating could well preserve the stability of mechanical structures of the composite and provide rapid transmission of Li-ions and electrons during the cycling tests, leading to high Li storage and enhancing the specific capacities and cycling stability (up to 561 mAh g^{-1} at 1 C after 100 cycles), which was higher than 30% compared to the pristine CuO anode.

5.4. Co_3O_4

Spinel Co_3O_4 is a transition metal oxide, which has been investigated as a competitive anode of LIBs [185–189] due to its high theoretical capacity (890 mAh g^{-1}) [185] and density (6.11 g cm^{-3}, about three times that of Gr). Like many conversion anodes, such as iron-based anodes, Co_3O_4 has poor electronic conductivity and suffers from severe volume change and particle aggregation during cycling, thus leading to poor stability performance. A thin PPy coating layer on the Co_3O_4 nanowires improved conductivity and acted as a buffer layer to relieve the strain induced by volume variation upon cycling. A Co_3O_4 coated with a PPy anode [190] displayed notably improved cycle performance with a reversible capacity of 700 mAh g^{-1} at 3 A g^{-1} after 500 cycles. In contrast, an uncoated Co_3O_4 nanowire

only showed 150 mAh g^{-1} after 100 cycles. The electrochemical performance of $CoCO_3$ anode materials of LIBs can also be improved by thin PPy coating layers [191].

5.5. $ZnFe_2O_4$

$ZnFe_2O_4$ is a low-cost, easy-to-prepare, abundant raw material, with a high theoretical capacity (1000 mAh g^{-1}). However, $ZnFe_2O_4$ anode materials, like other ternary mixed transition metal oxides, suffer from poor cycle stability and rate capability because of low electronic conductivity and significant volume expansion during (dis)charge (conversion reactions) processes. PDA, a bionic ionic permeable film, was coated on the surfaces of $ZnFe_2O_4$ particles by the self-polymerization of dopamine to accommodate the volume expansions [56]. $ZnFe_2O_4$@PDA composites delivered higher capacity and improved the rate capability of composites at high current densities compared to uncoated electrodes. PPy coating on one-dimensional $ZnFe_2O_4$ [53] also improved the rate capability of composite electrodes; more than two times capacity was retained at high current densities, 2 A g^{-1}, compared to the pristine electrodes.

A polymer coating also improves the electrochemical performance of the uncommon anodes on the anode particles, such as Bi_2S_3 by PEDOT [192], NiO by PANi [47], hard carbons by double coating with poly(dimethyldiallylammonium chloride) and poly(sodium-p-styrenesulfonate) for high rate anodes [60], aluminum by poly(ethylene oxide) [63], phosphorus anode by PPy [193], 3D porous conductive framework by hyperbranched polyol [194], and Sb_2S_3 by PPy [195].

5.6. Vanadium-Based Anodes

Wang et al. [196,197] reported the PPy surface polymer coating on vanadium-based anodes $Li_xV_2O_5$, which could stabilize the cycling capacity of the anode and improve the cycle life. With this approach, the PPy-coated anode delivers a better CE of ~86% after 40 cycles compared to a bare anode, whose initial capacity decreases to as low as a CE of ~8%. The cell performance of $LiMn_2O_4$/$LixV_2O_5$ has a specific capacity of 43 mAh g^{-1} at the voltage of 1.15 V [197]. The anode coated with a layer of PAN showed an improved electrochemical performance compared to the uncoated anode, with an initial capacity of 47 mAh g^{-1} and a CE of 80%.

Another interesting anode material is VS_2, a capable substitute for conventional carbon anode materials because of its high theoretical specific capacity. Nevertheless, this type of anode active material has not been applied in practical applications, since it suffers from significant capacity decay and poor cycle life. Zhou et al. [198] prepared VS_4 through a solvothermal method; this anode material offered some interesting properties, such as high sulfur content and one-dimensional structure. Three different polymers (PEDOT, PPY, and PANi) were reported as coatings on the VS_4 anode material surface to improve the electron conductivity, decrease the diffusion of polysulfides, and modify the electrode/electrolyte interface (Figure 10a). The VS_4 anode without polymer coating had a capacity of 100 mAh g^{-1}; PEDOT- and PPY-coated VS_4 had a specific capacity of 318 mAh g^{-1} (VS_4@PEDOT) and 448 mAh g^{-1} (VS_4@PPy), as shown in Figure 10b. Among these polymer coatings, VS_4@PANi exhibited a CE of 86% in the first cycle and a reversible capacity of about 755 mAh g^{-1} (100 mA g^{-1}) over 50 cycles. In comparison with PEDOT and PPy polymers, PANi exhibited better performances when coated on this anode material, which could be due to its strong interaction with VS_4 anode materials. Ding et al. studied PEDOT-PSS-coated VS_2 nanosheets prepared using an aqueous solution method [35]. The coated anode of 5VS_2@PEDOT-PSS delivered a higher reversible capacity of 569 mAh g^{-1} (0.1 A g^{-1}) after 100 cycles. Apart from VS_2 and VS_4 anodes, copper vanadate (CVO) is a promising anode material for LIBs due to its layered structure and excellent kinetics. The PEDOT:PSS-coated CuV_2O_6 nano-belts were prepared through a dip-and-dry method [199]. The electrochemical performance of CuV_2O_6/PEDOT:PSS and bare CVO anodes delivered a specific capacity of 915 mAh g^{-1} and 1142 mAh g^{-1}, respectively, in the first cycle. The reversible capacity after 100 cycles was 536.6 and 476.5 mAh g^{-1}, corresponding to coated

and uncoated CVO, respectively. The PEDOT:PSS coated on CVO anodes offered better electron and ion conductivity, fewer structural changes, and decreased unwanted side reactions during cycling.

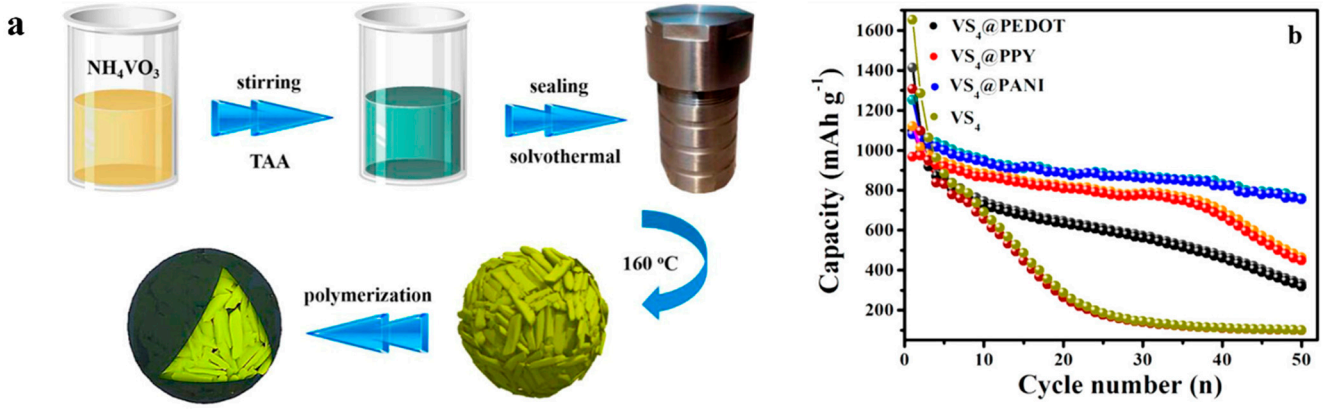

Figure 10. (**a**,**b**) Synthesis of the conductive-polymer-coated VS_4 sub-micro-spheres and the discharge profiles of VS_4@PEDOT, VS_4@PPY, and VS_4@PANi. Reproduced from Ref. [198] with permission from the American Chemical Society.

6. Summary and Outlook

LIBs technology provided a new door for energy storage for higher applications, especially in automotive EVs and HEVs, and stood out as an indispensable alternative for both present and future energy operations. In the past two decades, many studies on LIBs have been quite exciting, and more novel materials and strategies are being developed. There is a substantial demand for lightweight, reduced-size, space-efficient, low-cost, and high-capacity LIBs. This demand will continue to increase with technology maturation. Throughout the extensive material research and design, there should be an improvement in the development of various anode materials to enhance the capacity and cycle life of LIBs. This comprehensive review provides the various anode materials widely employed for LIBs and the polymer coating effects under investigation to increase their performance. The electrochemical reactions of LIBs were elaborated and overviewed with the advanced anode materials fabricated with a polymer coating.

Various coating strategies using polymer compounds are vital to improving the anode materials' performance and SEI concerns. Plenty of progress has been accomplished in developing high-performance anode materials for LIBs. However, further investigation is required into the supporting mechanisms that limit their performance to support the chemically stable materials' fabrication and development of easy processes for anode materials' production. We mainly discussed research activities regarding polymer coating with different anode materials and showed the achievements of various high-performance anode materials, i.e., intercalation anodes (Gr and titanium oxides), alloy anodes (Si-, Sn-, and Ge-based compounds), and conversion-type anodes (transition metal oxide compounds). Each category had promising features and capacities, but some drawbacks limit the optimal electrochemical performance of LIBs. Undoubtedly, substantial challenges occur for each component, requiring significant research efforts in various fields to open up their full potential for the high-performance anode materials. The Si- and Sn-based anodes are alloy-type materials and are the most attractive because of their high capacity. However, the main challenges are significant volume changes during cycling, which have limited the electrochemical performances, thus frustrating their implementation. In addition, some of these anode materials experience poor conductivity, affecting their low capacity. To overcome these challenges, the polymer coating approach demonstrated and showed excellent electrochemical performance in LIBs. Generally, the critical challenges for anode materials are poor cycle life and C-rate capability, low CE, unstable SEI, and high irreversible capacity. Polymer coating on the anode active material particles could solve some of these critical challenges, depending

on the anode material and specific polymer. For instance, in graphite anodes, the issue is Li plating with deep discharge at potentials near 0.0 V in a half cell (or fully charged for a full cell) and low initial CE. In Si-based anodes, the problem is volume expansion, resulting in unstable and thick SEI, poor cycling life, and low CE; transition metal oxides also have similar challenges. Therefore, a thin polymer coating (about 2–25 nm) can improve some of these issues via acting as an artificial SEI, and depending on the polymer, it could increase the conductivity of anode electrodes. Furthermore, maintaining the active anode materials' passivation and accommodating volume expansion during (de)lithiation processes improves the mechanical flexibility. Conductive polymers, such as PPy, PAN, and PEDOT, are frequently used because of their outstanding electrochemical properties. These polymers may also serve as a host for Li-ion (de)intercalation and deliver excellent electronic contact between the mass loading and the current collector.

A quantitative understanding of the mechanisms, polymer coating thickness, nanoscale design, and properties is still needed. To better understand the nature of the SEI layer produced with polymers, its impact on the CE needs to be fully considered. Notably, more advanced in situ/operando characterization techniques (such as TEM, X-ray photon spectroscopy (XPS), and X-ray diffraction (XRD)) and theoretical and simulation studies are necessary to explore the in-depth analysis of polymer coating microscopic processes that occur during (de)lithiation processes at the atomic and particle levels. Additionally, low-cost fabrication strategies must be developed for polymer coating on anodes with desirable performance. Polymer coating could enhance the interparticle connections of alloy anodes and lightweight production and application of high-capacity anode materials for LIBs. Future developments in the controllable thickness of various polymer coatings and control of SEI formulations, such as carbon nanotube anodes, Si anodes, and high-capacity Sn anodes, are promising advancements for the future of LIBs. This review provides a holistic view of recent innovations and advancements in the various kinds of polymer coatings for anode materials for LIBs. It also provides a broad view of the prospects that the field of battery technology holds for energy conversion, storage, and applications.

Funding: The authors thank the German Federal Ministry for Education and Research (BMBF) for the funding of research project EVanBatter (Reference No. 03XP0340B) from greenBatt-Cluster.

Data Availability Statement: Not applicable.

Conflicts of Interest: The authors declare no conflict of interest.

References

1. Kwade, A.; Haselrieder, W.; Leithoff, R.; Modlinger, A.; Dietrich, F.; Droeder, K. Current status and challenges for automotive battery production technologies. *Nat. Energy* **2018**, *3*, 290–300. [CrossRef]
2. Nitta, N.; Wu, F.; Lee, J.T.; Yushin, G. Li-ion battery materials: Present and future. *Mater. Today* **2015**, *18*, 252–264. [CrossRef]
3. Schmuch, R.; Wagner, R.; Hörpel, G.; Placke, T.; Winter, M. Performance and cost of materials for lithium-based rechargeable automotive batteries. *Nat. Energy* **2018**, *3*, 267–278. [CrossRef]
4. Cavers, H.; Molaiyan, P.; Abdollahifar, M.; Lassi, U.; Kwade, A. Perspectives on Improving the Safety and Sustainability of High Voltage Lithium-Ion Batteries Through the Electrolyte and Separator Region. *Adv. Energy Mater.* **2022**, *12*, 2200147. [CrossRef]
5. Peled, E.; Golodnitsky, D.; Ardel, G. Advanced model for solid electrolyte interphase electrodes in liquid and polymer electrolytes. *J. Electrochem. Soc.* **1997**, *144*, L208. [CrossRef]
6. Aurbach, D.; Markovsky, B.; Levi, M.D.; Levi, E.; Schechter, A.; Moshkovich, M.; Cohen, Y. New insights into the interactions between electrode materials and electrolyte solutions for advanced nonaqueous batteries. *J. Power Sources* **1999**, *81*, 95–111. [CrossRef]
7. Meda, U.S.; Lal, L.; Sushantha, M.; Garg, P. Solid Electrolyte Interphase (SEI), a boon or a bane for lithium batteries: A review on the recent advances. *J. Energy Storage* **2021**, *47*, 103564. [CrossRef]
8. Kim, J.; Chae, O.B.; Lucht, B.L. Perspective—structure and stability of the solid electrolyte interphase on silicon anodes of lithium-ion batteries. *J. Electrochem. Soc.* **2021**, *168*, 30521. [CrossRef]
9. Komaba, S.; Ozeki, T.; Okushi, K. Functional interface of polymer modified graphite anode. *J. Power Sources* **2009**, *189*, 197–203. [CrossRef]
10. Wang, C.; Wu, H.; Chen, Z.; McDowell, M.T.; Cui, Y.; Bao, Z. Self-healing chemistry enables the stable operation of silicon microparticle anodes for high-energy lithium-ion batteries. *Nat. Chem.* **2013**, *5*, 1042. [CrossRef]

11. Kim, J.-M.; Park, H.-S.; Park, J.-H.; Kim, T.-H.; Song, H.-K.; Lee, S.-Y. Conducting polymer-skinned electroactive materials of lithium-ion batteries: Ready for monocomponent electrodes without additional binders and conductive agents. *ACS Appl. Mater. Interfaces* **2014**, *6*, 12789–12797. [CrossRef] [PubMed]
12. Luo, J.; Wu, C.-E.; Su, L.-Y.; Huang, S.-S.; Fang, C.-C.; Wu, Y.-S.; Chou, J.; Wu, N.-L. A proof-of-concept graphite anode with a lithium dendrite suppressing polymer coating. *J. Power Sources* **2018**, *406*, 63–69. [CrossRef]
13. Carter, R.; Parker, J.F.; Sassin, M.B.; Klein, E.J.; Wolak, M.A.; Love, C.T.; Long, J.W. Initiated Chemical Vapor Deposition of Ultrathin Polymer Coatings at Graphite Electrodes for Enhanced Performance in Li-Ion Batteries. *J. Electrochem. Soc.* **2020**, *167*, 60510. [CrossRef]
14. Li, C.; Zhang, H.P.; Fu, L.J.; Liu, H.; Wu, Y.P.; Rahm, E.; Holze, R.; Wu, H.Q. Cathode materials modified by surface coating for lithium ion batteries. *Electrochim. Acta* **2006**, *51*, 3872–3883. [CrossRef]
15. Mauger, A.; Julien, C. Surface modifications of electrode materials for lithium-ion batteries: Status and trends. *Ionics* **2014**, *20*, 751–787. [CrossRef]
16. Oriňáková, R.; Fedorková, A.; Oriňák, A. Effect of PPy/PEG conducting polymer film on electrochemical performance of LiFePO4 cathode material for Li-ion batteries. *Chem. Pap.* **2013**, *67*, 860–875. [CrossRef]
17. Li, F.-S.; Wu, Y.-S.; Chou, J.; Winter, M.; Wu, N.-L. A Mechanically Robust and Highly Ion-Conductive Polymer-Blend Coating for High-Power and Long-Life Lithium-Ion Battery Anodes. *Adv. Mater.* **2015**, *27*, 130–137. [CrossRef]
18. Cao, Z.; Xu, P.; Zhai, H.; Du, S.; Mandal, J.; Dontigny, M.; Zaghib, K.; Yang, Y. Ambient-Air Stable Lithiated Anode for Rechargeable Li-Ion Batteries with High Energy Density. *Nano Lett.* **2016**, *16*, 7235–7240. [CrossRef]
19. Liu, Y.; Zhou, G.; Liu, K.; Cui, Y. Design of Complex Nanomaterials for Energy Storage: Past Success and Future Opportunity. *Acc. Chem. Res.* **2017**, *50*, 2895–2905. [CrossRef]
20. Wang, F.; Chen, G.; Zhang, N.; Liu, X.; Ma, R. Engineering of carbon and other protective coating layers for stabilizing silicon anode materials. *Carbon Energy* **2019**, *1*, 219–245. [CrossRef]
21. Zhou, H.; Yu, S.; Liu, H.; Liu, P. Protective coatings for lithium metal anodes: Recent progress and future perspectives. *J. Power Sources* **2020**, *450*, 227632. [CrossRef]
22. Fedorov, R.G.; Maletti, S.; Heubner, C.; Michaelis, A.; Ein-Eli, Y. Molecular Engineering Approaches to Fabricate Artificial Solid-Electrolyte Interphases on Anodes for Li-Ion Batteries: A Critical Review. *Adv. Energy Mater.* **2021**, *11*, 2101173. [CrossRef]
23. Pham, Q.-T.; Chern, C.-S. Applications of polymers in lithium-ion batteries with enhanced safety and cycle life. *J. Polym. Res.* **2022**, *29*, 124. [CrossRef]
24. Chen, Z.; Soltani, A.; Chen, Y.; Zhang, Q.; Davoodi, A.; Hosseinpour, S.; Peukert, W.; Liu, W. Emerging Organic Surface Chemistry for Si Anodes in Lithium-Ion Batteries: Advances, Prospects, and Beyond. *Adv. Energy Mater.* **2022**, *12*, 2200924. [CrossRef]
25. Lu, J.; Chen, Z.; Pan, F.; Cui, Y.; Amine, K. High-performance anode materials for rechargeable lithium-ion batteries. *Electrochem. Energy Rev.* **2018**, *1*, 35–53. [CrossRef]
26. Yuan, L.; Wang, J.; Chew, S.Y.; Chen, J.; Guo, Z.P.; Zhao, L.; Konstantinov, K.; Liu, H.-K. Synthesis and characterization of SnO_2–polypyrrole composite for lithium-ion battery. *J. Power Sources* **2007**, *174*, 1183–1187. [CrossRef]
27. Shao, Q.-G.; Chen, W.-M.; Wang, Z.-H.; Qie, L.; Yuan, L.-X.; Zhang, W.-X.; Hu, X.-L.; Huang, Y.-H. SnO_2-based composite coaxial nanocables with multi-walled carbon nanotube and polypyrrole as anode materials for lithium-ion batteries. *Electrochem. Commun.* **2011**, *13*, 1431–1434. [CrossRef]
28. Liu, R.; Li, D.; Wang, C.; Li, N.; Li, Q.; Lü, X.; Spendelow, J.S.; Wu, G. Core–shell structured hollow SnO_2–polypyrrole nanocomposite anodes with enhanced cyclic performance for lithium-ion batteries. *Nano Energy* **2014**, *6*, 73–81. [CrossRef]
29. Cao, Z.; Yang, H.; Dou, P.; Wang, C.; Zheng, J.; Xu, X. Synthesis of three-dimensional hollow SnO_2@PPy nanotube arrays via template-assisted method and chemical vapor-phase polymerization as high performance anodes for lithium-ion batteries. *Electrochim. Acta* **2016**, *209*, 700–708. [CrossRef]
30. Guan, B.Y.; Yu, L.; Li, J.; Lou, X.W. A universal cooperative assembly-directed method for coating of mesoporous TiO_2 nanoshells with enhanced lithium storage properties. *Sci. Adv.* **2016**, *2*, e1501554. [CrossRef]
31. Liu, Y.; Tang, D.; Zhong, H.; Zhang, Q.; Yang, J.; Zhang, L. Facile synthesis of nanostructured Li4Ti5O12/PEDOT:PSS composite as anode material for lithium-ion batteries. *RSC Adv.* **2016**, *6*, 95512–95517. [CrossRef]
32. Sun, X.; Lu, X.; Huang, S.; Xi, L.; Liu, L.; Liu, B.; Weng, Q.; Zhang, L.; Schmidt, O.G. Reinforcing Germanium Electrode with Polymer Matrix Decoration for Long Cycle Life Rechargeable Lithium Ion Batteries. *ACS Appl. Mater. Interfaces* **2017**, *9*, 38556–38566. [CrossRef]
33. Xu, D.; Wang, P.; Yang, R. Conducting polythiophene-wrapped $Li_4Ti_5O_{12}$ spinel anode material for ultralong cycle-life Li-ion batteries. *Ceram. Int.* **2017**, *43*, 4712–4715. [CrossRef]
34. Zhou, Y.; Jin, X.; Ni, J.; Zhang, S.; Yang, J.; Liu, P.; Wang, Z.; Lei, J. Evaporation induced uniform polypyrrole coating on CuO arrays for free-standing high lithium storage anode. *J. Solid State Electrochem.* **2019**, *23*, 1829–1836. [CrossRef]
35. Ding, Z.; Zhang, Q.; Chen, Y.; Liu, G.; Xin, X.; He, H.; Cai, B.; Wu, J.; Yao, X. PEDOT-PSS coated VS2 nanosheet anodes for high rate and ultrastable lithium-ion batteries. *New J. Chem.* **2019**, *43*, 1681–1687. [CrossRef]
36. Tolganbek, N.; Mentbayeva, A.; Serik, N.; Batyrgali, N.; Naizakarayev, M.; Kanamura, K.; Bakenov, Z. Design and preparation of thin film gel polymer electrolyte for 3D Li-ion battery. *J. Power Sources* **2021**, *493*, 229686. [CrossRef]
37. Zhang, Z.; Wu, D.; Jiang, L.; Liang, F.; Rui, Y.; Tang, B. One-step synthesis based on non-aqueous sol-gel conductive polymer-coated SnO_2 nanoparticles as advanced anode materials for lithium-ion batteries. *J. Alloys Compd.* **2022**, *899*, 163274. [CrossRef]

38. Abdollahifar, M.; Vinograd, A.; Lu, C.-Y.; Chang, S.-J.; Müller, J.; Frankenstein, L.; Placke, T.; Kwade, A.; Winter, M.; Chao, C.-Y. Enabling Long-Cycling Life of Si-on-Graphite Composite Anodes via Fabrication of a Multifunctional Polymeric Artificial Solid–Electrolyte Interphase Protective Layer. *ACS Appl. Mater. Interfaces* **2022**, *34*, 38824–38834. [CrossRef]
39. Seo, J.; Hyun, S.; Moon, J.; Lee, J.Y.; Kim, C. High Performance of a Polydopamine-Coated Graphite Anode with a Stable SEI Layer. *ACS Appl. Energy Mater.* **2022**, *5*, 5610–5616. [CrossRef]
40. Liu, Y.; Matsumura, T.; Imanishi, N.; Hirano, A.; Ichikawa, T.; Takeda, Y. Preparation and Characterization of Si/C Composite Coated with Polyaniline as Novel Anodes for Li-Ion Batteries. *Electrochem. Solid State Lett.* **2005**, *8*, A599. [CrossRef]
41. Xiao, W.; Chen, J.S.; Lu, Q.; Lou, X.W. Porous spheres assembled from polythiophene (PTh)-coated ultrathin MnO_2 nanosheets with enhanced lithium storage capabilities. *J. Phys. Chem. C* **2010**, *114*, 12048–12051. [CrossRef]
42. Jeong, J.-M.; Choi, B.G.; Lee, S.C.; Lee, K.G.; Chang, S.-J.; Han, Y.-K.; Lee, Y.B.; Lee, H.U.; Kwon, S.; Lee, G. Hierarchical hollow spheres of Fe_2O_3@ polyaniline for lithium ion battery anodes. *Adv. Mater.* **2013**, *25*, 6250–6255. [CrossRef]
43. Han, F.; Li, D.; Li, W.-C.; Lei, C.; Sun, Q.; Lu, A.-H. Nanoengineered Polypyrrole-Coated Fe_2O_3@ C Multifunctional Composites with an Improved Cycle Stability as Lithium-Ion Anodes. *Adv. Funct. Mater.* **2013**, *23*, 1692–1700. [CrossRef]
44. Du, F.-H.; Li, B.; Fu, W.; Xiong, Y.-J.; Wang, K.-X.; Chen, J.-S. Surface binding of polypyrrole on porous Silicon hollow nanospheres for Li-ion battery anodes with high structure Stability. *Adv. Mater.* **2014**, *26*, 6145–6150. [CrossRef]
45. Luo, L.; Zhao, P.; Yang, H.; Liu, B.; Zhang, J.-G.; Cui, Y.; Yu, G.; Zhang, S.; Wang, C.-M. Surface Coating Constraint Induced Self-Discharging of Silicon Nanoparticles as Anodes for Lithium Ion Batteries. *Nano Lett.* **2015**, *15*, 7016–7022. [CrossRef]
46. Yin, Z.; Fan, W.; Ding, Y.; Li, J.; Guan, L.; Zheng, Q. Shell Structure Control of PPy-Modified CuO Composite Nanoleaves for Lithium Batteries with Improved Cyclic Performance. *ACS Sustain. Chem. Eng.* **2015**, *3*, 507–517. [CrossRef]
47. Ma, H.; Liu, X.; Zhang, D.; Xiang, J. Synthesis of polyaniline shell on nickel oxide nanoflake arrays for enhanced lithium ion storage. *Mater. Res. Bull.* **2017**, *96*, 301–305. [CrossRef]
48. Gu, H.; Chen, F.; Liu, C.; Qian, J.; Ni, M.; Liu, T. Scalable fabrication of core-shell structured $Li_4Ti_5O_{12}$/PPy particles embedded in N-doped graphene networks as advanced anode for lithium-ion batteries. *J. Power Sources* **2017**, *369*, 42–49. [CrossRef]
49. Attia, E.N.; Hassan, F.M.; Li, M.; Batmaz, R.; Elkamel, A.; Chen, Z. Tailoring the chemistry of blend copolymers boosting the electrochemical performance of Si-based anodes for lithium ion batteries. *J. Mater. Chem. A* **2017**, *5*, 24159–24167. [CrossRef]
50. Fu, R.; Nie, P.; Shi, M.; Wang, J.; Jiang, J.; Zhang, Y.; Wu, Y.; Fang, S.; Dou, H.; Zhang, X. Rigid Polyimide Buffering Layer Enabling Silicon Nanoparticles Prolonged Cycling Life for Lithium Storage. *ACS Appl. Energy Mater.* **2018**, *1*, 948–955. [CrossRef]
51. Shen, B.H.; Wang, S.; Tenhaeff, W.E. Ultrathin conformal polycyclosiloxane films to improve silicon cycling stability. *Sci. Adv.* **2019**, *5*, eaaw4856. [CrossRef]
52. Shi, W.; Wu, H.B.; Baucom, J.; Li, X.; Ma, S.; Chen, G.; Lu, Y. Covalently Bonded Si–Polymer Nanocomposites Enabled by Mechanochemical Synthesis as Durable Anode Materials. *ACS Appl. Mater. Interfaces* **2020**, *12*, 39127–39134. [CrossRef]
53. Hou, L.; Bao, R.; kionga Denis, D.; Sun, X.; Zhang, J.; uz Zaman, F.; Yuan, C. Synthesis of ultralong $ZnFe_2O_4$@ polypyrrole nanowires with enhanced electrochemical Li-storage behaviors for lithium-ion batteries. *Electrochim. Acta* **2019**, *306*, 198–208. [CrossRef]
54. Li, Z.-F.; Zhang, H.; Liu, Q.; Liu, Y.; Stanciu, L.; Xie, J. Novel pyrolyzed polyaniline-grafted silicon nanoparticles encapsulated in graphene sheets as Li-ion battery anodes. *ACS Appl. Mater. Interfaces* **2014**, *6*, 5996–6002. [CrossRef]
55. Chen, X.; Cao, Z.; Xing, L.; Liao, Y.; Qiu, Y.; Li, W. Improved Li-storage performance with PEDOT-decorated MnO_2 nanoboxes. *Nanoscale* **2017**, *9*, 18467–18473. [CrossRef]
56. Yue, H.; Du, T.; Wang, Q.; Shi, Z.; Dong, H.; Cao, Z.; Qiao, Y.; Yin, Y.; Xing, R.; Yang, S. Biomimetic Synthesis of Polydopamine Coated ZnFe2O4 Composites as Anode Materials for Lithium-Ion Batteries. *ACS Omega* **2018**, *3*, 2699–2705. [CrossRef]
57. Kim, Y.S.; Kim, S.H.; Kim, G.; Heo, S.; Mun, J.; Han, S.; Jung, H.; Kyoung, Y.K.; Yun, D.J.; Baek, W.J.; et al. Protective Oxide Coating for Ionic Conductive Solid Electrolyte Interphase. *ACS Appl. Mater. Interfaces* **2016**, *8*, 30980–30984. [CrossRef]
58. Li, F.-S.; Wu, Y.-S.; Chou, J.; Wu, N.-L. A dimensionally stable and fast-discharging graphite–silicon composite Li-ion battery anode enabled by electrostatically self-assembled multifunctional polymer-blend coating. *Chem. Commun.* **2015**, *51*, 8429–8431. [CrossRef]
59. Liu, J.; Xu, J.; Chen, Y.; Sun, W.; Zhou, X.; Ke, J. Synthesis and electrochemical performance of a PEDOT: pSS@ Ge composite as the anode materials for lithium-ion batteries. *Int. J. Electrochem. Sci.* **2019**, *14*, 359–370. [CrossRef]
60. Wu, Y.S.; Lyu, P.R. Double-Coated Hard Carbon as an Anode Material for High C-Rate Lithium Ion Batteries. *Mater. Sci. Forum* **2018**, *921*, 105–110. [CrossRef]
61. Nieradko, M.; Eskandarian, L.; Semenikhin, O.A. Aluminum anodes coated with polymer electrolyte show improved reversibility and cycling ability in Li-Ion batteries. *Electrochim. Acta* **2019**, *327*, 135023. [CrossRef]
62. Abdollahifar, M.; Doose, S.; Cavers, H.; Kwade, A. Graphite Recycling from End-of-Life Lithium-Ion Batteries: Processes and Applications. *Adv. Mater. Technol.* **2022**, 2200368. [CrossRef]
63. Abdollahifar, M.; Molaiyan, P.; Lassi, U.; Wu, N.L.; Kwade, A. Multifunctional behaviour of graphite in lithium–sulfur batteries. *Renew. Sustain. Energy Rev.* **2022**, *169*, 112948. [CrossRef]
64. Zhang, H.; Yang, Y.; Ren, D.; Wang, L.; He, X. Graphite as anode materials: Fundamental mechanism, recent progress and advances. *Energy Storage Mater.* **2021**, *36*, 147–170. [CrossRef]
65. Zhou, Y.F.; Xie, S.; Chen, C.H. Pyrolytic polyurea encapsulated natural graphite as anode material for lithium ion batteries. *Electrochim. Acta* **2005**, *50*, 4728–4735. [CrossRef]

66. Pan, Q.; Wang, H.; Jiang, Y. Natural graphite modified with nitrophenyl multilayers as anode materials for lithium ion batteries. *J. Mater. Chem.* **2007**, *17*, 329–334. [CrossRef]
67. Chao, D.; Xia, X.; Liu, J.; Fan, Z.; Ng, C.F.; Lin, J.; Zhang, H.; Shen, Z.X.; Fan, H.J. A V2O5/conductive-polymer core/shell nanobelt array on three-dimensional graphite foam: A high-rate, ultrastable, and freestanding cathode for lithium-ion batteries. *Adv. Mater.* **2014**, *26*, 5794–5800. [CrossRef]
68. Asenbauer, J.; Eisenmann, T.; Kuenzel, M.; Kazzazi, A.; Chen, Z.; Bresser, D. The success story of graphite as a lithium-ion anode material–fundamentals, remaining challenges, and recent developments including silicon (oxide) composites. *Sustain. Energy Fuels* **2020**, *4*, 5387–5416. [CrossRef]
69. Ui, K.; Kikuchi, S.; Mikami, F.; Kadoma, Y.; Kumagai, N. Improvement of electrochemical characteristics of natural graphite negative electrode coated with polyacrylic acid in pure propylene carbonate electrolyte. *J. Power Sources* **2007**, *173*, 518–521. [CrossRef]
70. Shi, Q.; Liu, W.; Qu, Q.; Gao, T.; Wang, Y.; Liu, G.; Battaglia, V.S.; Zheng, H. Robust solid/electrolyte interphase on graphite anode to suppress lithium inventory loss in lithium-ion batteries. *Carbon* **2017**, *111*, 291–298. [CrossRef]
71. Müller, J.; Abdollahifar, M.; Vinograd, A.; Nöske, M.; Nowak, C.; Chang, S.-J.; Placke, T.; Haselrieder, W.; Winter, M.; Kwade, A. Si-on-Graphite fabricated by fluidized bed process for high-capacity anodes of Li-ion batteries. *Chem. Eng. J.* **2021**, *407*, 126603. [CrossRef]
72. Müller, J.; Abdollahifar, M.; Doose, S.; Michalowski, P.; Wu, N.-L.; Kwade, A. Effects of carbon coating on calendered nano-silicon graphite composite anodes of LiB. *J. Power Sources* **2022**, *548*, 232000. [CrossRef]
73. Komaba, S.; Okushi, K.; Groult, H. Polyacrylate as modifier for graphite/electrolyte interface. *ECS Trans.* **2008**, *11*, 63. [CrossRef]
74. Nie, M.; Abraham, D.P.; Seo, D.M.; Chen, Y.; Bose, A.; Lucht, B.L. Role of solution structure in solid electrolyte interphase formation on graphite with LiPF6 in propylene carbonate. *J. Phys. Chem. C* **2013**, *117*, 25381–25389. [CrossRef]
75. Xu, K.; Zhang, S.; Poese, B.A.; Jow, T.R. Lithium bis (oxalato) borate stabilizes graphite anode in propylene carbonate. *Electrochem. Solid State Lett.* **2002**, *5*, A259. [CrossRef]
76. Luo, J.; Fang, C.-C.; Wu, N.-L. High polarity poly (vinylidene difluoride) thin coating for dendrite-free and high-performance lithium metal anodes. *Adv. Energy Mater.* **2018**, *8*, 1701482. [CrossRef]
77. Lau, K.K.S.; Gleason, K.K. Initiated chemical vapor deposition (iCVD) of poly (alkyl acrylates): An experimental study. *Macromolecules* **2006**, *39*, 3688–3694. [CrossRef]
78. Martin, T.P.; Lau, K.K.S.; Chan, K.; Mao, Y.; Gupta, M.; O'Shaughnessy, W.S.; Gleason, K.K. Initiated chemical vapor deposition (iCVD) of polymeric nanocoatings. *Surf. Coat. Technol.* **2007**, *201*, 9400–9405. [CrossRef]
79. Subramanian, V.; Karki, A.; Gnanasekar, K.I.; Eddy, F.P.; Rambabu, B. Nanocrystalline TiO_2 (anatase) for Li-ion batteries. *J. Power Sources* **2006**, *159*, 186–192. [CrossRef]
80. Zhang, H.; Yang, Y.; Xu, H.; Wang, L.; Lu, X.; He, X. $Li_4Ti_5O_{12}$ spinel anode: Fundamentals and advances in rechargeable batteries. *InfoMat* **2022**, *4*, e12228. [CrossRef]
81. Chen, Z.; Belharouak, I.; Sun, Y.-K.; Amine, K. Titanium-based anode materials for safe lithium-ion batteries. *Adv. Funct. Mater.* **2013**, *23*, 959–969. [CrossRef]
82. Yi, T.-F.; Zhu, Y.-R.; Tao, W.; Luo, S.; Xie, Y.; Li, X.-F. Recent advances in the research of MLi_2Ti6O_{14} (M= 2Na, Sr, Ba, Pb) anode materials for Li-ion batteries. *J. Power Sources* **2018**, *399*, 26–41. [CrossRef]
83. Lai, C.; Li, G.R.; Dou, Y.Y.; Gao, X.P. Mesoporous polyaniline or polypyrrole/anatase TiO_2 nanocomposite as anode materials for lithium-ion batteries. *Electrochim. Acta* **2010**, *55*, 4567–4572. [CrossRef]
84. Zheng, H.; Ncube, N.M.; Raju, K.; Mphahlele, N.; Mathe, M. The effect of polyaniline on TiO_2 nanoparticles as anode materials for lithium ion batteries. *SpringerPlus* **2016**, *5*, 630. [CrossRef]
85. Lee, J.-K.; Kung, M.C.; Trahey, L.; Missaghi, M.N.; Kung, H.H. Nanocomposites derived from phenol-functionalized Si nanoparticles for high performance lithium ion battery anodes. *Chem. Mater.* **2009**, *21*, 6–8. [CrossRef]
86. Li, J.; Huang, J. A nanofibrous polypyrrole/silicon composite derived from cellulose substance as the anode material for lithium-ion batteries. *Chem. Commun.* **2015**, *51*, 14590–14593. [CrossRef]
87. Yasar-Inceoglu, O.; Zhong, L.; Mangolini, L. Core/shell silicon/polyaniline particles via in-flight plasma-induced polymerization. *J. Phys. D Appl. Phys.* **2015**, *48*, 314009. [CrossRef]
88. Mu, T.; Zhao, Y.; Zhao, C.; Holmes, N.G.; Lou, S.; Li, J.; Li, W.; He, M.; Sun, Y.; Du, C.; et al. Stable Silicon Anodes by Molecular Layer Deposited Artificial Zincone Coatings. *Adv. Funct. Mater.* **2021**, *31*, 2010526. [CrossRef]
89. Liu, Z.; Yu, Q.; Zhao, Y.; He, R.; Xu, M.; Feng, S.; Li, S.; Zhou, L.; Mai, L. Silicon oxides: A promising family of anode materials for lithium-ion batteries. *Chem. Soc. Rev.* **2019**, *48*, 285–309. [CrossRef]
90. Chou, C.-Y.; Hwang, G.S. On the origin of the significant difference in lithiation behavior between silicon and germanium. *J. Power Sources* **2014**, *263*, 252–258. [CrossRef]
91. Zheng, H.; Fang, S.; Tong, Z.; Dou, H.; Zhang, X. Porous Silicon@Polythiophene Core–Shell Nanospheres for Lithium-Ion Batteries. *Part. Part. Syst. Charact.* **2016**, *33*, 75–81. [CrossRef]
92. Wu, H.; Cui, Y. Designing nanostructured Si anodes for high energy lithium ion batteries. *Nano Today* **2012**, *7*, 414–429. [CrossRef]
93. Jin, Y.; Zhu, B.; Lu, Z.; Liu, N.; Zhu, J. Challenges and recent progress in the development of Si anodes for lithium-ion battery. *Adv. Energy Mater.* **2017**, *7*, 1700715. [CrossRef]

94. Wang, G.X.; Ahn, J.H.; Yao, J.; Bewlay, S.; Liu, H.K. Nanostructured Si–C composite anodes for lithium-ion batteries. *Electrochem. Commun.* **2004**, *6*, 689–692. [CrossRef]
95. Dou, F.; Shi, L.; Chen, G.; Zhang, D. Silicon/carbon composite anode materials for lithium-ion batteries. *Electrochem. Energy Rev.* **2019**, *2*, 149–198. [CrossRef]
96. Wu, H.; Yu, G.; Pan, L.; Liu, N.; McDowell, M.T.; Bao, Z.; Cui, Y. Stable Li-ion battery anodes by in-situ polymerization of conducting hydrogel to conformally coat silicon nanoparticles. *Nat. Commun.* **2013**, *4*, 1943. [CrossRef]
97. Huang, Y.; Li, H.; Wang, Z.; Zhu, M.; Pei, Z.; Xue, Q.; Huang, Y.; Zhi, C. Nanostructured polypyrrole as a flexible electrode material of supercapacitor. *Nano Energy* **2016**, *22*, 422–438. [CrossRef]
98. Song, H.-K.; Palmore, G.T.R. Redox-active polypyrrole: Toward polymer-based batteries. *Adv. Mater.* **2006**, *18*, 1764–1768. [CrossRef]
99. Wang, G.X.; Yang, L.; Chen, Y.; Wang, J.Z.; Bewlay, S.; Liu, H.K. An investigation of polypyrrole-$LiFePO_4$ composite cathode materials for lithium-ion batteries. *Electrochim. Acta* **2005**, *50*, 4649–4654. [CrossRef]
100. Fu, Y.; Su, Y.-S.; Manthiram, A. Sulfur-polypyrrole composite cathodes for lithium-sulfur batteries. *J. Electrochem. Soc.* **2012**, *159*, A1420. [CrossRef]
101. Karimi, A.; Kazeminezhad, I.; Naderi, L.; Shahrokhian, S. Construction of a Ternary Nanocomposite, Polypyrrole/Fe–Co Sulfide-Reduced Graphene Oxide/Nickel Foam, as a Novel Binder-Free Electrode for High-Performance Asymmetric Supercapacitors. *J. Phys. Chem. C* **2020**, *124*, 4393–4407. [CrossRef]
102. Guo, Z.P.; Wang, J.Z.; Liu, H.K.; Dou, S.X. Study of silicon/polypyrrole composite as anode materials for Li-ion batteries. *J. Power Sources* **2005**, *146*, 448–451. [CrossRef]
103. Chew, S.Y.; Guo, Z.P.; Wang, J.Z.; Chen, J.; Munroe, P.; Ng, S.H.; Zhao, L.; Liu, H.K. Novel nano-silicon/polypyrrole composites for lithium storage. *Electrochem. Commun.* **2007**, *9*, 941–946. [CrossRef]
104. Magasinski, A.; Dixon, P.; Hertzberg, B.; Kvit, A.; Ayala, J.; Yushin, G. High-performance lithium-ion anodes using a hierarchical bottom-up approach. *Nat. Mater.* **2010**, *9*, 353–358. [CrossRef] [PubMed]
105. Kovalenko, I.; Zdyrko, B.; Magasinski, A.; Hertzberg, B.; Milicev, Z.; Burtovyy, R.; Luzinov, I.; Yushin, G. A major constituent of brown algae for use in high-capacity Li-ion batteries. *Science* **2011**, *334*, 75–79. [CrossRef]
106. Chan, C.K.; Peng, H.; Liu, G.; McIlwrath, K.; Zhang, X.F.; Huggins, R.A.; Cui, Y. High-performance lithium battery anodes using silicon nanowires. *Nat. Nanotechnol.* **2008**, *3*, 31–35. [CrossRef] [PubMed]
107. Xu, J.-C.; Liu, W.-M.; Li, H.-L. Titanium dioxide doped polyaniline. *Mater. Sci. Eng. C* **2005**, *25*, 444–447. [CrossRef]
108. Mu, G.; Ding, Z.; Mu, D.; Wu, B.; Bi, J.; Zhang, L.; Yang, H.; Wu, H.; Wu, F. Hierarchical void structured Si/PANi/C hybrid anode material for high-performance lithium-ion batteries. *Electrochim. Acta* **2019**, *300*, 341–348. [CrossRef]
109. Pan, S.; Han, J.; Wang, Y.; Li, Z.; Chen, F.; Guo, Y.; Han, Z.; Xiao, K.; Yu, Z.; Yu, M. Integrating SEI into Layered Conductive Polymer Coatings for Ultrastable Silicon Anodes. *Adv. Mater.* **2022**, *34*, 2203617. [CrossRef]
110. Yoon, J.H.; Lee, G.; Li, P.; Baik, H.; Yi, G.-R.; Park, J.H. Expandable crosslinked polymer coatings on silicon nanoparticle anode toward high-rate and long-cycle-life lithium-ion battery. *Appl. Surf. Sci.* **2022**, *571*, 151294. [CrossRef]
111. Wang, Q.; Zhu, M.; Chen, G.; Dudko, N.; Li, Y.; Liu, H.; Shi, L.; Wu, G.; Zhang, D. High-Performance Microsized Si Anodes for Lithium-Ion Batteries: Insights into the Polymer Configuration Conversion Mechanism. *Adv. Mater.* **2022**, *34*, 2109658. [CrossRef] [PubMed]
112. Gu, H.; Wang, Y.; Zeng, Y.; Yu, M.; Liu, T.; Chen, J.; Wang, K.; Xie, J.; Li, L. Boosting Cyclability and Rate Capability of SiOx via Dopamine Polymerization-Assisted Hybrid Graphene Coating for Advanced Lithium-Ion Batteries. *ACS Appl. Mater. Interfaces* **2022**, *14*, 17388–17395. [CrossRef] [PubMed]
113. Gao, X.-W.; Wang, J.-Z.; Chou, S.-L.; Liu, H.-K. Synthesis and electrochemical performance of LiV_3O_8/polyaniline as cathode material for the lithium battery. *J. Power Sources* **2012**, *220*, 47–53. [CrossRef]
114. Gittleson, F.S.; Hwang, J.; Sekol, R.C.; Taylor, A.D. Polymer coating of vanadium oxide nanowires to improve cathodic capacity in lithium batteries. *J. Mater. Chem. A* **2013**, *1*, 7979–7984. [CrossRef]
115. Lee, Y.-S.; Shin, W.-K.; Kannan, A.G.; Koo, S.M.; Kim, D.-W. Improvement of the Cycling Performance and Thermal Stability of Lithium-Ion Cells by Double-Layer Coating of Cathode Materials with Al_2O_3 Nanoparticles and Conductive Polymer. *ACS Appl. Mater. Interfaces* **2015**, *7*, 13944–13951. [CrossRef] [PubMed]
116. Park, J.-H.; Cho, J.-H.; Kim, J.-S.; Shim, E.-G.; Lee, S.-Y. High-voltage cell performance and thermal stability of nanoarchitectured polyimide gel polymer electrolyte-coated $LiCoO_2$ cathode materials. *Electrochim. Acta* **2012**, *86*, 346–351. [CrossRef]
117. Jiang, B.; He, Y.; Li, B.; Zhao, S.; Wang, S.; He, Y.-B.; Lin, Z. Polymer-Templated Formation of Polydopamine-Coated SnO_2 Nanocrystals: Anodes for Cyclable Lithium-Ion Batteries. *Angew. Chem. Int. Ed.* **2017**, *56*, 1869–1872. [CrossRef]
118. Fan, X.; Jiang, A.; Dou, P.; Ma, D.; Xu, X. Three-dimensional ultrathin Sn/polypyrrole nanosheet network as high performance lithium-ion battery anode. *RSC Adv.* **2014**, *4*, 52074–52082. [CrossRef]
119. Li, S.; Wang, C.; Yu, J.; Han, Y.; Lu, Z. Understanding the role of conductive polymer in thermal lithiation and battery performance of Li-Sn alloy anode. *Energy Storage Mater.* **2019**, *20*, 7–13. [CrossRef]
120. Cao, Z.; Meng, H.; Dou, P.; Wang, C.; Zheng, J.; Xu, X. Effects of solid polymer electrolyte coating on the composition and morphology of the solid electrolyte interphase on Sn anodes. *J. Solid State Electrochem.* **2017**, *21*, 955–966. [CrossRef]
121. Cui, L.; Shen, J.; Cheng, F.; Tao, Z.; Chen, J. SnO_2 nanoparticles@ polypyrrole nanowires composite as anode materials for rechargeable lithium-ion batteries. *J. Power Sources* **2011**, *196*, 2195–2201. [CrossRef]

122. Zhou, M.; Liu, Y.; Chen, J.; Yang, X. Double shelled hollow SnO_2/polymer microsphere as a high-capacity anode material for superior reversible lithium ion storage. *J. Mater. Chem. A* **2015**, *3*, 1068–1076. [CrossRef]
123. Li, S.; Wi, T.-U.; Ji, M.; Cui, Z.; Lee, H.-W.; Lu, Z. The Role of Polymer and Inorganic Coatings to Enhance Interparticle Connections Diagnosed by In Situ Techniques. *Nano Lett.* **2021**, *21*, 1530–1537. [CrossRef] [PubMed]
124. Li, B.; Bi, R.; Yang, M.; Gao, W.; Wang, J. Coating conductive polypyrrole layers on multiple shells of hierarchical SnO_2 spheres and their enhanced cycling stability as lithium-ion battery anode. *Appl. Surf. Sci.* **2022**, *586*, 152836. [CrossRef]
125. Sher Shah, M.S.A.; Muhammad, S.; Park, J.H.; Yoon, W.-S.; Yoo, P.J. Incorporation of PEDOT:PSS into SnO_2/reduced graphene oxide nanocomposite anodes for lithium-ion batteries to achieve ultra-high capacity and cyclic stability. *RSC Adv.* **2015**, *5*, 13964–13971. [CrossRef]
126. Li, H.; Zhang, B.; Ou, X.; Zhou, Q.; Wang, C.; Peng, C.; Zhang, J. Core-Shell Structure of SnO_2@C/PEDOT: PSS Microspheres with Dual Protection Layers for Enhanced Lithium Storage Performance. *ChemElectroChem* **2019**, *6*, 2182–2188. [CrossRef]
127. Guo, J.; Chen, L.; Wang, G.; Zhang, X.; Li, F. In situ synthesis of SnO_2–Fe_2O_3@ polyaniline and their conversion to SnO_2–Fe_2O_3@ C composite as fully reversible anode material for lithium-ion batteries. *J. Power Sources* **2014**, *246*, 862–867. [CrossRef]
128. Fan, X.; Dou, P.; Jiang, A.; Ma, D.; Xu, X. One-Step Electrochemical Growth of a Three-Dimensional Sn–Ni@PEO Nanotube Array as a High Performance Lithium-Ion Battery Anode. *ACS Appl. Mater. Interfaces* **2014**, *6*, 22282–22288. [CrossRef]
129. Gowda, S.R.; Reddy, A.L.M.; Shaijumon, M.M.; Zhan, X.; Ci, L.; Ajayan, P.M. Conformal coating of thin polymer electrolyte layer on nanostructured electrode materials for three-dimensional battery applications. *Nano Lett.* **2011**, *11*, 101–106. [CrossRef]
130. Dou, P.; Cao, Z.; Zheng, J.; Wang, C.; Xu, X. Solid polymer electrolyte coating three-dimensional Sn/Ni bimetallic nanotube arrays for high performance lithium-ion battery anodes. *J. Alloys Compd.* **2016**, *685*, 690–698. [CrossRef]
131. Xiao, X.; Li, X.; Zheng, S.; Shao, J.; Xue, H.; Pang, H. Nanostructured germanium anode materials for advanced rechargeable batteries. *Adv. Mater. Interfaces* **2017**, *4*, 1600798. [CrossRef]
132. Hu, Z.; Zhang, S.; Zhang, C.; Cui, G. High performance germanium-based anode materials. *Coord. Chem. Rev.* **2016**, *326*, 34–85. [CrossRef]
133. Li, X.; Yang, Z.; Fu, Y.; Qiao, L.; Li, D.; Yue, H.; He, D. Germanium anode with excellent lithium storage performance in a germanium/lithium–cobalt oxide lithium-ion battery. *ACS Nano* **2015**, *9*, 1858–1867. [CrossRef]
134. Seng, K.H.; Park, M.-H.; Guo, Z.P.; Liu, H.K.; Cho, J. Self-assembled germanium/carbon nanostructures as high-power anode material for the lithium-ion battery. *Angew. Chem.* **2012**, *124*, 5755–5759. [CrossRef]
135. Liu, X.; Wu, X.-Y.; Chang, B.; Wang, K.-X. Recent progress on germanium-based anodes for lithium ion batteries: Efficient lithiation strategies and mechanisms. *Energy Storage Mater.* **2020**, *30*, 146–169. [CrossRef]
136. Zhao, J.; Zhang, Y.; Wang, Y.; Li, H.; Peng, Y. The application of nanostructured transition metal sulfides as anodes for lithium ion batteries. *J. Energy Chem.* **2018**, *27*, 1536–1554. [CrossRef]
137. Nam, K.-H.; Jeon, K.-J.; Park, C.-M. Layered germanium phosphide-based anodes for high-performance lithium-and sodium-ion batteries. *Energy Storage Mater.* **2019**, *17*, 78–87. [CrossRef]
138. Liu, Q.; Liu, C.; Li, Z.; Liang, Q.; Zhu, B.; Chai, J.; Cheng, X.; Zheng, P.; Zheng, Y.; Liu, Z. Layered Tin Phosphide Composites as Promising Anodes for Lithium-Ion Batteries. *ACS Appl. Energy Mater.* **2021**, *4*, 11306–11313. [CrossRef]
139. Tseng, K.-W.; Huang, S.-B.; Chang, W.-C.; Tuan, H.-Y. Synthesis of mesoporous germanium phosphide microspheres for high-performance lithium-ion and sodium-ion battery anodes. *Chem. Mater.* **2018**, *30*, 4440–4447. [CrossRef]
140. Lin, H.-P.; Chen, K.-T.; Chang, C.-B.; Tuan, H.-Y. Aluminum phosphide as a high-performance lithium-ion battery anode. *J. Power Sources* **2020**, *465*, 228262. [CrossRef]
141. Chae, S.; Park, S.; Ahn, K.; Nam, G.; Lee, T.; Sung, J.; Kim, N.; Cho, J. Gas phase synthesis of amorphous silicon nitride nanoparticles for high-energy LIBs. *Energy Environ. Sci.* **2020**, *13*, 1212–1221. [CrossRef]
142. De Guzman, R.C.; Yang, J.; Cheng, M.M.-C.; Salley, S.O.; Ng, K.S. High capacity silicon nitride-based composite anodes for lithium ion batteries. *J. Mater. Chem. A* **2014**, *2*, 14577–14584. [CrossRef]
143. Zhang, M.; Qiu, Y.; Han, Y.; Guo, Y.; Cheng, F. Three-dimensional tungsten nitride nanowires as high performance anode material for lithium ion batteries. *J. Power Sources* **2016**, *322*, 163–168. [CrossRef]
144. Li, C.; Zhu, L.; Qi, S.; Ge, W.; Ma, W.; Zhao, Y.; Huang, R.; Xu, L.; Qian, Y. Ultrahigh-areal-capacity battery anodes enabled by free-standing vanadium nitride@ N-doped carbon/graphene architecture. *ACS Appl. Mater. Interfaces* **2020**, *12*, 49607–49616. [CrossRef]
145. Zhu, X.; Zhu, Y.; Murali, S.; Stoller, M.D.; Ruoff, R.S. Nanostructured reduced graphene oxide/Fe_2O_3 composite as a high-performance anode material for lithium ion batteries. *ACS Nano* **2011**, *5*, 3333–3338. [CrossRef]
146. Jiang, T.; Bu, F.; Feng, X.; Shakir, I.; Hao, G.; Xu, Y. Porous Fe_2O_3 nanoframeworks encapsulated within three-dimensional graphene as high-performance flexible anode for lithium-ion battery. *ACS Nano* **2017**, *11*, 5140–5147. [CrossRef]
147. Reddy, M.V.; Yu, T.; Sow, C.-H.; Shen, Z.X.; Lim, C.T.; Subba Rao, G.V.; Chowdari, B.V.R. α-Fe_2O_3 nanoflakes as an anode material for Li-ion batteries. *Adv. Funct. Mater.* **2007**, *17*, 2792–2799. [CrossRef]
148. Jiang, Y.; Zhang, D.; Li, Y.; Yuan, T.; Bahlawane, N.; Liang, C.; Sun, W.; Lu, Y.; Yan, M. Amorphous Fe_2O_3 as a high-capacity, high-rate and long-life anode material for lithium ion batteries. *Nano Energy* **2014**, *4*, 23–30. [CrossRef]
149. He, C.; Wu, S.; Zhao, N.; Shi, C.; Liu, E.; Li, J. Carbon-encapsulated Fe_3O_4 nanoparticles as a high-rate lithium ion battery anode material. *ACS Nano* **2013**, *7*, 4459–4469. [CrossRef]

150. Zhou, G.; Wang, D.-W.; Li, F.; Zhang, L.; Li, N.; Wu, Z.-S.; Wen, L.; Lu, G.Q.; Cheng, H.-M. Graphene-wrapped Fe_3O_4 anode material with improved reversible capacity and cyclic stability for lithium ion batteries. *Chem. Mater.* **2010**, *22*, 5306–5313. [CrossRef]
151. Kopuklu, B.B.; Tasdemir, A.; Gursel, S.A.; Yurum, A. High stability graphene oxide aerogel supported ultrafine Fe_3O_4 particles with superior performance as a Li-ion battery anode. *Carbon* **2021**, *174*, 158–172. [CrossRef]
152. Salimi, P.; Norouzi, O.; Pourhosseini, S.E.M. Two-step synthesis of nanohusk Fe_3O_4 embedded in 3D network pyrolytic marine biochar for a new generation of anode materials for Lithium-Ion batteries. *J. Alloys Compd.* **2019**, *786*, 930–937. [CrossRef]
153. Ma, J.; Kong, Y.; Liu, S.; Li, Y.; Jiang, J.; Zhou, Q.; Huang, Y.; Han, S. Flexible phosphorus-doped graphene/metal–organic framework-derived porous Fe_2O_3 anode for lithium-ion battery. *ACS Appl. Energy Mater.* **2020**, *3*, 11900–11906. [CrossRef]
154. Park, J.; Yoo, H.; Choi, J. 3D ant-nest network of α-Fe_2O_3 on stainless steel for all-in-one anode for Li-ion battery. *J. Power Sources* **2019**, *431*, 25–30. [CrossRef]
155. Wang, Z.; Luan, D.; Madhavi, S.; Li, C.M.; Lou, X.W.D. α-Fe_2O_3 nanotubes with superior lithium storage capability. *Chem. Commun.* **2011**, *47*, 8061–8063. [CrossRef]
156. Zhou, W.; Cheng, C.; Liu, J.; Tay, Y.Y.; Jiang, J.; Jia, X.; Zhang, J.; Gong, H.; Hng, H.H.; Yu, T. Epitaxial growth of branched α-Fe_2O_3/SnO_2 nano-heterostructures with improved lithium-ion battery performance. *Adv. Funct. Mater.* **2011**, *21*, 2439–2445. [CrossRef]
157. Wang, Z.; Luan, D.; Madhavi, S.; Hu, Y.; Lou, X.W.D. Assembling carbon-coated α-Fe_2O_3 hollow nanohorns on the CNT backbone for superior lithium storage capability. *Energy Environ. Sci.* **2012**, *5*, 5252–5256. [CrossRef]
158. Xu, X.; Cao, R.; Jeong, S.; Cho, J. Spindle-like mesoporous α-Fe_2O_3 anode material prepared from MOF template for high-rate lithium batteries. *Nano Lett.* **2012**, *12*, 4988–4991. [CrossRef]
159. Zou, Y.; Kan, J.; Wang, Y. Fe_2O_3-graphene rice-on-sheet nanocomposite for high and fast lithium ion storage. *J. Phys. Chem. C* **2011**, *115*, 20747–20753. [CrossRef]
160. Liu, J.; Zhou, W.; Lai, L.; Yang, H.; Lim, S.H.; Zhen, Y.; Yu, T.; Shen, Z.; Lin, J. Three dimensionals α-Fe_2O_3/polypyrrole (Ppy) nanoarray as anode for micro lithium ion batteries. *Nano Energy* **2013**, *2*, 726–732. [CrossRef]
161. Applestone, D.; Manthiram, A. Cu 6 Sn 5–TiC–C nanocomposite alloy anodes with high volumetric capacity for lithium ion batteries. *RSC Adv.* **2012**, *2*, 5411–5417. [CrossRef]
162. Zhao, J.; Zhang, S.; Liu, W.; Du, Z.; Fang, H. Fe_3O_4/PPy composite nanospheres as anode for lithium-ion batteries with superior cycling performance. *Electrochim. Acta* **2014**, *121*, 428–433. [CrossRef]
163. Wang, X.; Liu, Y.; Han, H.; Zhao, Y.; Ma, W.; Sun, H. Polyaniline coated Fe_3O_4 hollow nanospheres as anode materials for lithium ion batteries. *Sustain. Energy Fuels* **2017**, *1*, 915–922. [CrossRef]
164. Wei, W.; Cui, X.; Chen, W.; Ivey, D.G. Manganese oxide-based materials as electrochemical supercapacitor electrodes. *Chem. Soc. Rev.* **2011**, *40*, 1697–1721. [CrossRef]
165. Reddy, A.L.M.; Shaijumon, M.M.; Gowda, S.R.; Ajayan, P.M. Coaxial MnO_2/carbon nanotube array electrodes for high-performance lithium batteries. *Nano Lett.* **2009**, *9*, 1002–1006. [CrossRef]
166. Gu, X.; Yue, J.; Li, L.; Xue, H.; Yang, J.; Zhao, X. General synthesis of MnOx (MnO_2, Mn_2O_3, Mn_3O_4, MnO) hierarchical microspheres as lithium-ion battery anodes. *Electrochim. Acta* **2015**, *184*, 250–256. [CrossRef]
167. Wang, D.; Wang, L.; Liang, G.; Li, H.; Liu, Z.; Tang, Z.; Liang, J.; Zhi, C. A superior δ-MnO_2 cathode and a self-healing Zn-δ-MnO_2 battery. *ACS Nano* **2019**, *13*, 10643–10652. [CrossRef]
168. Zeng, Y.; Zhang, X.; Meng, Y.; Yu, M.; Yi, J.; Wu, Y.; Lu, X.; Tong, Y. Achieving Ultrahigh Energy Density and Long Durability in a Flexible Rechargeable Quasi-Solid-State Zn–MnO_2 Battery. *Adv. Mater.* **2017**, *29*, 1700274. [CrossRef]
169. Weng, Y.-T.; Huang, T.-Y.; Lim, C.-H.; Shao, P.-S.; Hy, S.; Kuo, C.-Y.; Cheng, J.-H.; Hwang, B.-J.; Lee, J.-F.; Wu, N.-L. An unexpected large capacity of ultrafine manganese oxide as a sodium-ion battery anode. *Nanoscale* **2015**, *7*, 20075–20081. [CrossRef]
170. Wang, L.; Cao, X.; Xu, L.; Chen, J.; Zheng, J. Transformed akhtenskite MnO_2 from Mn_3O_4 as cathode for a rechargeable aqueous zinc ion battery. *ACS Sustain. Chem. Eng.* **2018**, *6*, 16055–16063. [CrossRef]
171. Akbari Garakani, M.; Abouali, S.; Cui, J.; Kim, J.-K. In situ TEM study of lithiation into a PPy coated α-MnO_2/graphene foam freestanding electrode. *Mater. Chem. Front.* **2018**, *2*, 1481–1488. [CrossRef]
172. Muhammad, N.; Yasin, G.; Li, A.; Chen, Y.; Saleem, H.M.; Liu, R.; Li, D.; Sun, Y.; Zheng, S.; Chen, X. Volumetric buffering of manganese dioxide nanotubes by employing 'as is' graphene oxide: An approach towards stable metal oxide anode material in lithium-ion batteries. *J. Alloys Compd.* **2020**, *842*, 155803. [CrossRef]
173. Abdollahifar, M.; Liu, H.-W.; Lin, C.-H.; Weng, Y.-T.; Sheu, H.-S.; Lee, J.-F.; Lu, M.-L.; Liao, Y.-F.; Wu, N.-L. Enabling Extraordinary Rate Performance for Poorly Conductive Oxide Pseudocapacitors. *Energy Environ. Mater.* **2020**, *3*, 405–413. [CrossRef]
174. Abdollahifar, M.; Huang, S.-S.; Lin, Y.-H.; Sheu, H.-S.; Lee, J.-F.; Lu, M.-L.; Liao, Y.-F.; Wu, N.-L. Tetragonal $LiMn_2O_4$ as dual-functional pseudocapacitor-battery electrode in aqueous Li-ion electrolytes. *J. Power Sources* **2019**, *412*, 545–551. [CrossRef]
175. Abdollahifar, M.; Huang, S.-S.; Lin, Y.-H.; Lin, Y.-C.; Shih, B.-Y.; Sheu, H.-S.; Liao, Y.-F.; Wu, N.-L. High-performance carbon-coated ZnMn2O4 nanocrystallite supercapacitors with tailored microstructures enabled by a novel solution combustion method. *J. Power Sources* **2018**, *378*, 90–97. [CrossRef]
176. Wang, C.; Higgins, D.; Wang, F.; Li, D.; Liu, R.; Xia, G.; Li, N.; Li, Q.; Xu, H.; Wu, G. Controlled synthesis of micro/nanostructured CuO anodes for lithium-ion batteries. *Nano Energy* **2014**, *9*, 334–344. [CrossRef]

177. Wang, Z.; Zhang, Y.; Xiong, H.; Qin, C.; Zhao, W.; Liu, X. Yucca fern shaped CuO nanowires on Cu foam for remitting capacity fading of Li-ion battery anodes. *Sci. Rep.* **2018**, *8*, 6530. [CrossRef]
178. Zhu, C.; Chao, D.; Sun, J.; Bacho, I.M.; Fan, Z.; Ng, C.F.; Xia, X.; Huang, H.; Zhang, H.; Shen, Z.X. Enhanced lithium storage performance of CuO nanowires by coating of graphene quantum dots. *Adv. Mater. Interfaces* **2015**, *2*, 1400499. [CrossRef]
179. Yin, D.; Huang, G.; Na, Z.; Wang, X.; Li, Q.; Wang, L. CuO nanorod arrays formed directly on Cu foil from MOFs as superior binder-free anode material for lithium-ion batteries. *ACS Energy Lett.* **2017**, *2*, 1564–1570. [CrossRef]
180. Wang, X.; Tang, D.-M.; Li, H.; Yi, W.; Zhai, T.; Bando, Y.; Golberg, D. Revealing the conversion mechanism of CuO nanowires during lithiation–delithiation by in situ transmission electron microscopy. *Chem. Commun.* **2012**, *48*, 4812–4814. [CrossRef]
181. Wu, R.; Qian, X.; Yu, F.; Liu, H.; Zhou, K.; Wei, J.; Huang, Y. MOF-templated formation of porous CuO hollow octahedra for lithium-ion battery anode materials. *J. Mater. Chem. A* **2013**, *1*, 11126–11129. [CrossRef]
182. Chen, X.; Zhang, N.; Sun, K. Facile fabrication of CuO mesoporous nanosheet cluster array electrodes with super lithium-storage properties. *J. Mater. Chem.* **2012**, *22*, 13637–13642. [CrossRef]
183. Xue, X.; Deng, P.; Yuan, S.; Nie, Y.; He, B.; Xing, L.; Zhang, Y. CuO/PVDF nanocomposite anode for a piezo-driven self-charging lithium battery. *Energy Environ. Sci.* **2013**, *6*, 2615–2620. [CrossRef]
184. Yin, Z.; Ding, Y.; Zheng, Q.; Guan, L. CuO/polypyrrole core–shell nanocomposites as anode materials for lithium-ion batteries. *Electrochem. Commun.* **2012**, *20*, 40–43. [CrossRef]
185. Yan, N.; Hu, L.; Li, Y.; Wang, Y.; Zhong, H.; Hu, X.; Kong, X.; Chen, Q. Co_3O_4 nanocages for high-performance anode material in lithium-ion batteries. *J. Phys. Chem. C* **2012**, *116*, 7227–7235. [CrossRef]
186. Wang, Y.; Wang, B.; Xiao, F.; Huang, Z.; Wang, Y.; Richardson, C.; Chen, Z.; Jiao, L.; Yuan, H. Facile synthesis of nanocage Co_3O_4 for advanced lithium-ion batteries. *J. Power Sources* **2015**, *298*, 203–208. [CrossRef]
187. Li, Y.; Tan, B.; Wu, Y. Mesoporous Co_3O_4 nanowire arrays for lithium ion batteries with high capacity and rate capability. *Nano Lett.* **2008**, *8*, 265–270. [CrossRef]
188. Liu, Y.; Mi, C.; Su, L.; Zhang, X. Hydrothermal synthesis of Co_3O_4 microspheres as anode material for lithium-ion batteries. *Electrochim. Acta* **2008**, *53*, 2507–2513. [CrossRef]
189. Huang, G.; Xu, S.; Lu, S.; Li, L.; Sun, H. Micro-/nanostructured Co_3O_4 anode with enhanced rate capability for lithium-ion batteries. *ACS Appl. Mater. Interfaces* **2014**, *6*, 7236–7243. [CrossRef]
190. Zhan, L.; Chen, H.; Fang, J.; Wang, S.; Ding, L.-X.; Li, Z.; Ashman, P.J.; Wang, H. Coaxial Co_3O_4@polypyrrole core-shell nanowire arrays for high performance lithium ion batteries. *Electrochim. Acta* **2016**, *209*, 192–200. [CrossRef]
191. Ding, Z.; Yao, B.; Feng, J.; Zhang, J. Enhanced rate performance and cycling stability of a $CoCO_3$–polypyrrole composite for lithium ion battery anodes. *J. Mater. Chem. A* **2013**, *1*, 11200–11209. [CrossRef]
192. Mukkabla, R.; Deepa, M.; Srivastava, A.K. Enhanced Lithium-Ion Storage Capability of a Bismuth Sulfide/Graphene Oxide/Poly(3,4-ethylenedioxythiophene) Composite. *ChemPhysChem* **2015**, *16*, 3242–3253. [CrossRef]
193. Li, X.; Han, X.; Liu, R.; Zhang, S.; Zhang, Y.; Cao, Y.; Wang, X.; Wang, R.; Yang, Z.; Sun, J. Tannic acid-polypyrrole multifunctional coating layer enhancing the interface effect and efficient Li-ion transport of a phosphorus anode. *Nanoscale* **2022**, *14*, 3625–3631. [CrossRef] [PubMed]
194. Wang, H.; Chen, W.; Chen, Z.; Zhang, C.; Jiang, L.; Yu, F. A lithiophilic hyperbranched polymer-decorated three-dimensional carbon skeleton boosting highly reversible lithium metal anode. *Colloids Surf. A Physicochem. Eng. Asp.* **2022**, *647*, 129104. [CrossRef]
195. Yin, W.; Chai, W.; Wang, K.; Ye, W.; Rui, Y.; Tang, B. A highly Meso@Microporous carbon-supported Antimony sulfide nanoparticles coated by conductive polymer for high-performance lithium and sodium ion batteries. *Electrochim. Acta* **2019**, *321*, 134699. [CrossRef]
196. Wang, H.; Zeng, Y.; Huang, K.; Liu, S.; Chen, L. Improvement of cycle performance of lithium ion cell LiMn2O4/LixV2O5 with aqueous solution electrolyte by polypyrrole coating on anode. *Electrochim. Acta* **2007**, *52*, 5102–5107. [CrossRef]
197. Wang, H.; Huang, K.; Zeng, Y.; Zhao, F.; Chen, L. Stabilizing Cyclability of an Aqueous Lithium-Ion Battery LiNi1/3Mn1/3Co1/3O2/Li x V2O5 by Polyaniline Coating on the Anode. *Electrochem. Solid State Lett.* **2007**, *10*, A199. [CrossRef]
198. Zhou, Y.; Li, Y.; Yang, J.; Tian, J.; Xu, H.; Yang, J.; Fan, W. Conductive Polymer-Coated VS4 Submicrospheres As Advanced Electrode Materials in Lithium-Ion Batteries. *ACS Appl. Mater. Interfaces* **2016**, *8*, 18797–18805. [CrossRef]
199. Zhang, S.; Hu, R. Synthesis and electrochemical performance of CuV2O6/PEDOT:PSS composite nanobelts as anode materials for lithium-ion batteries. *Mater. Lett.* **2016**, *176*, 131–134. [CrossRef]